



Antibacterial Activity of Silver Nanoparticles Composed by Fruit Aqueous Extract of *Abelmoschus esculentus* (L.) Moench Alone or in Combination with Antibiotics

Ali A. Shareef^{*1}, Fadhil J. Farhan² & Fulla A. A. Alriyahee¹

¹Department of Biology, College of Education for Pure Sciences, University of Basrah, Iraq

²College of Marine Science, University of Basrah, Iraq

*Corresponding author email: A.A.S.: aliaboud547@gmail.com; F.J.F.: fadhil.farhan@uobasrah.edu.iq;
F.A.A.A.: fulla.abed@uobasrah.edu.iq

Received 24th May 2023; Accepted 18th Sept 2023; Available online 29th December 2023

Abstract: Nanoparticle applications are growing due to the unique properties that nanoparticles possess, which have gained the attention of researchers, and one of these applications is the use of inhibiting antibiotic-resistant bacteria. The current work aims to biosynthesize silver nanoparticles from the fruits of the okra plant *Abelmoschus esculentus* (L.) Moench and test their antibacterial activity alone or in combination with some antibiotics. The creation of silver nanoparticles was confirmed by altering the colour of the mixture from light green to dark brown, in addition to employing spectroscopic methods to prove and explain the production of these particles, such as UV-vis, FTIR, XRD, and EDX. Scanning electron microscopy (SEM) was used to determine the shape and sizes of the particles created in the current study. The synthesized silver nanoparticles were tested alone or in combination with some antibiotics for their ability to inhibit four species of antibiotic-resistant MDR bacteria, three of which were Gram-negative and the fourth was Gram-positive bacteria. The results demonstrated that these bacteria were inhibited when using nanoparticles at all concentrations alone or in combination with antibiotics. AgNPs were found to be more effective against Gram-positive bacteria than Gram-negative bacteria. Therefore, *Staphylococcus auricularis* (8F) was the most sensitive bacteria at all concentrations, while *Escherichia coli* (3R) was the most resistant. The results of the combination of AgNPs with some antibiotics revealed that the best synergy was recorded when AgNPs mixed with Amoxicillin clavulanate against all species of Gram-negative bacteria, followed by ciprofloxacin, Ampicillin, and Fosfomycin.

Keywords: AgNPs, Antibacterial Activity, Antibiotics combination.

Introduction

Many biologists, chemists, and researchers have observed a significant increase in nanotechnology research, driven by the unique properties and diverse applications of metal nanoparticles. These nanoparticles have shown their ability to kill or inhibit pathogenic bacteria that cause disease in humans and animals (Vanlalveni *et al.*, 2021). Almudhafar & Al-Hamdani (2022) demonstrated that silver

nanoparticles made from plant extracts can suppress pathogenic bacteria and cancer cells. Nanotechnology is a rapidly emerging field that focuses on the fabricating nanoparticles ranging in size from 1 to 100 nanometers. Its broad-ranging applications extend multiple scientific disciplines, including medicine, environmental science, agriculture, and many others. One of the key advantages of

nanotechnology lies in its ability to significantly increase the surface area to volume, leading to a range of unique characteristics. Nanoparticles can be fabricated in several ways, which include chemical, physical, optical, and bio-manufacturing approaches. Biological methods offer distinct advantages over other techniques, as they are financially inexpensive, environmentally friendly, and require lower power in manufacturing (Zahoor, *et al.*, 2021). In addition to being environmentally friendly and low-cost, the production of nanoparticles from plant extracts is capable of suppressing cancer cells (Al-Musawi & Al-Sadi, 2021). Silver nanoparticles have many medical applications such as their use in drug delivery and incorporation of silver nanoparticles in ointments to treat bacterial infections in burn wounds. In biological methods also utilize silver nanoparticles to deliver genes to target sites in genetic engineering experiments. Bio-manufacturing of silver nanoparticles involves the utilization of living organisms such as bacteria, fungi, algae, and plants, thus avoiding the use of dangerous and toxic chemicals for humans or the environment (Habeb Rahuman *et al.*, 2022). Plants, especially aqueous extracts obtained from leaves, stems, fruits, etc., can be used in the green synthesis of silver nanoparticles. This is attributed to the abundance of biomolecules present in plants that actively contribute in the biosynthesis of these nanoparticles (Vanlalveni *et al.*, 2021).

Okra plant (Baima in Iraq) *Abelmoschus esculentus* (L.) Moench (Syn: *Hibiscus esculentus* L.) belongs to the family Malvaceae. Plant taxonomists disagreed about the origins of the okra plant. Some assert that the plant originated from Asia or Africa while others state that it originated from India. There are indications that it was planted in the Nile Valley before the discovery of America.

However, the most accepted view is that the plant has its wild origins in Nubia, Kordofan, Sennar, Abyssinia, and the Baar-el-Abiad (Townsend & Guest, 1980). Okra plant is cultivated in most Iraqi cities, and there are four varieties whose cultivation spreads from one region to another. These varieties are classified based on the size of the fruit, as well as the shape and height of the stem. The specific varieties are Bathrah, Bethrah, Hindiya, and Musalliah. The fruits of the okra plant are used as a staple food in various regions of Iraq and can be consumed after being boiled or made as a broth after adding meat, spices, and curry. Okra fruits contain protein, fats, minerals, fiber, carbohydrates, calcium, phosphorus, iron, and others, in addition to vitamins and citric acid. (Chakravarty, 1976).

The current study aimed to use the aqueous extract of the fruits of the *A. esculentus* plant in order to reduce silver nitrate to silver nanoparticles, since the aqueous extract is taken from a plant that is eaten as a main meal in Iraq, in addition to that it is non-toxic.

Materials and Methods

Preparation of plant extract

Plant extract was done according to Shareef *et al.* (2022) with some modification briefly: The fruits of *A. esculentus* plant were obtained from the local markets of Basra Governorate, washed with tap water to remove impurities, boiled for 10 minutes, and left to cool at room temperature. The filtrate was collected after filtration and divided into two parts. The first section was examined by a GC/MS analysis to identify the active compounds of the extract, and the second section was prepared for manufacturing silver nanoparticles. Both were kept at 4°C until use.

AgNPs synthesis

Green synthesis of AgNPs was done according to Shareef *et al.* (2022) with some modification briefly: Silver nanoparticles were synthesized by using the aqueous extract of *A. esculentus* fruits as follows: The aqueous extract obtained from the previous paragraph was diluted with distilled water at a ratio of 1:1, since the solution is viscous. The silver nitrate, with a final reaction concentration of 1 mM, was dissolved with 200 ml of diluted extract in a 500 ml conical flask and incubated at room temperature. The reaction mixture was periodically monitored until the colour of the reaction mixture changed from light green to dark brown due to the formation of silver nanoparticles. The silver nanoparticles produced in the current investigation were purified by washing them three times with DDw. The silver nanoparticles were dried at room temperature and stored in the refrigerator as a powder until subsequent studies.

Characterization of AgNPs

The formation of AgNPs was monitored using the following instruments:

UV-Visible spectroscopy analysis

The peaks of silver nanoparticles were detected using ultraviolet (SN: YB010282003058 (China)) spectrophotometer analysis between 350 and 800 nm.

Fourier Transform Infrared Spectroscopy (FTIR)

To determine the bioactive compounds present in plant extract and silver nanoparticles solution, an FTIR spectrum was performed utilizing potassium bromide powder by using Schemadzu Affinity apparatus (Japan) with an absorbance of 500-4000 Cm^{-1} .

X-ray diffraction analysis (XRD) analysis

XRD (Burker, USA) analysis was utilized to determine the crystal structure of the silver nanoparticles created in the current study.

Scanning Electron Microscope (SEM)

SEM (FEI Nova NanoSEM 450) apparatus was used to determine the size and shape of the particles created for the current study. The energy dispersive spectroscopy (EDX) study along with the SEM examination served as the basis for determining the chemical composition of the nanoparticles.

Antibacterial activity of AgNPs

In order to measure the inhibitory effect of silver nanoparticles, three human pathogenic Gram-negative bacteria (*Alcaligenes faecalis* (2R), *Escherichia coli* (3R), and *Escherichia coli* (11F)), and one Gram positive (*Staphylococcus auricularis* (8F)) were identified by morphological, biochemical, and molecular methods by using *16SrDNA* gene, were used in the current study. Antibacterial activity of AgNPs was done by Agar well diffusion method as follows: Bacterial inoculum was done by 24-hour bacteria were suspended in a solution of 0.5 McFarland standards and spread on the surface of Mueller Hinton agar Petri dishes after being spread with a cotton swab. Different concentrations of silver nanoparticles were prepared by dissolving 0.010 g of AgNPs in 10 ml of dimethyl sulfoxide (DMSO) to obtain a concentration of 1000 $\mu\text{g}\cdot\text{ml}^{-1}$ and then a series of dilutions was done to obtain 500, 250, 125, and 62.5 $\mu\text{g}/\text{ml}$ concentrations, Then wells were prepared with a cork borer of 6 mm in diameter, filled with varying concentrations of silver nanoparticles. Petri dishes were incubated at 37°C for 24 hours. Antibacterial activity of AgNPs were detected by measuring the inhibition zone around each well in mm. The clear zone around the wells represents no

growth of bacteria i.e. Bacteria were inhibited. (Shareef *et al.*, 2022).

Detection of the synergistic action of AgNPs with antibiotics

The synergistic activity of the synthesized silver nanoparticles by the aqueous extract of *A. esculentus* fruits was done by adding 10 microliters of silver nanoparticles at five concentrations were prepared in the same technique as in the preceding paragraph (1000, 500, 250, 125, and 62.5 µg/ml) to the following antibiotics (Ampicillin, Azithromycin, Aztreonam, Ceftazidime, Chloramphenicol, Ciprofloxacin, Clindamycin, Colistin, Fosfomycin, Gentamicin, Linezolid, Meropenem, Methicillin, Nitrofurantoin, Penicillin, Piperacillin, Piperacillin-tazobactam, Rifampicin, Teicoplanin, Tetracycline, Trimethoprim-Sulfamethoxazole, and Vancomycin) against three Gram-negative bacteria (*Alcaligenes faecalis* (2R), *Escherichia coli* (3R), and *Escherichia coli* (11F)), and one Gram positive (*Staphylococcus auricularis* (8F)) by using the standard disc diffusion method to detect the synergistic activity of silver nanoparticles with antibiotics. Following a 24-hour incubation period at 37 °C, the diameter of the inhibition zone was measured in millimeters to assess the synergistic effects of the nanoparticles when added to the antibiotics by using the equation synergism % = $\frac{B-A}{A} \times 100$, where A is the diameter of the antibiotic's inhibition zone and B is the diameter of the antibiotic's inhibition zone + AgNPs (Moteriya *et al.*, 2017). The fractional inhibitory concentration index (FICI) was calculated according to the following formula (Odds, 2003).

$$FICI = \frac{\text{AgNPs growth inhibition alone} + \text{antibiotic growth inhibition alone}}{\text{growth inhibition of combined agents}}$$

Where: FICI ≤ 0.5 (synergy) or FIC > 0.5 < 4, (additive), and FIC > 4 (antagonism).

Statistical analysis

The results recorded in this study was analyzed statistically using Statistical Package for the Social Sciences (SPSS) version -24, Chi-square with P ≤ 0.05. to measure statistically significant.

Results & Discussion

GC/MS analysis results

The current study recorded the presence of 123 compounds in the aqueous extract of the *A. esculentus* plant (Fig.1, Table1), and the most abundant compounds were: 2,3-Butanediol with RT% (15.5204) is a glycol compound (Secondary alcohol) produced naturally by many organisms such as in the roots of *Ruta graveolens*, *Zea mays*, and *Bacillus polymyxa*. It was also used in World War II as an alternative to plastic (Norman, 1993). The second compound is Methanamine, N-methoxy-RT% (7.5124); this compound was isolated from the green alga *Chlorella pyrenoidosa*, which is one of the amino compounds that are involved in the synthesis of proteins, Lethane RT% (4.7457), 2-Methoxy-4-vinylphenol RT% (4.0701) it is a phenolic compound that is a member of the guaiacol class of phenols. In addition, it had a pheromone nature and a secondary metabolite in many plants (Schuphan, 1974). Shareef *et al.* (2022) reported the compound 5-Hydroxymethylfurfural (reducing sugars) when they analyzed pollen grain aqueous extract of *Typha domingensis* Pers. According to Tian *et al.* (2022), these compounds are responsible for the green synthesis of silver nanoparticles.

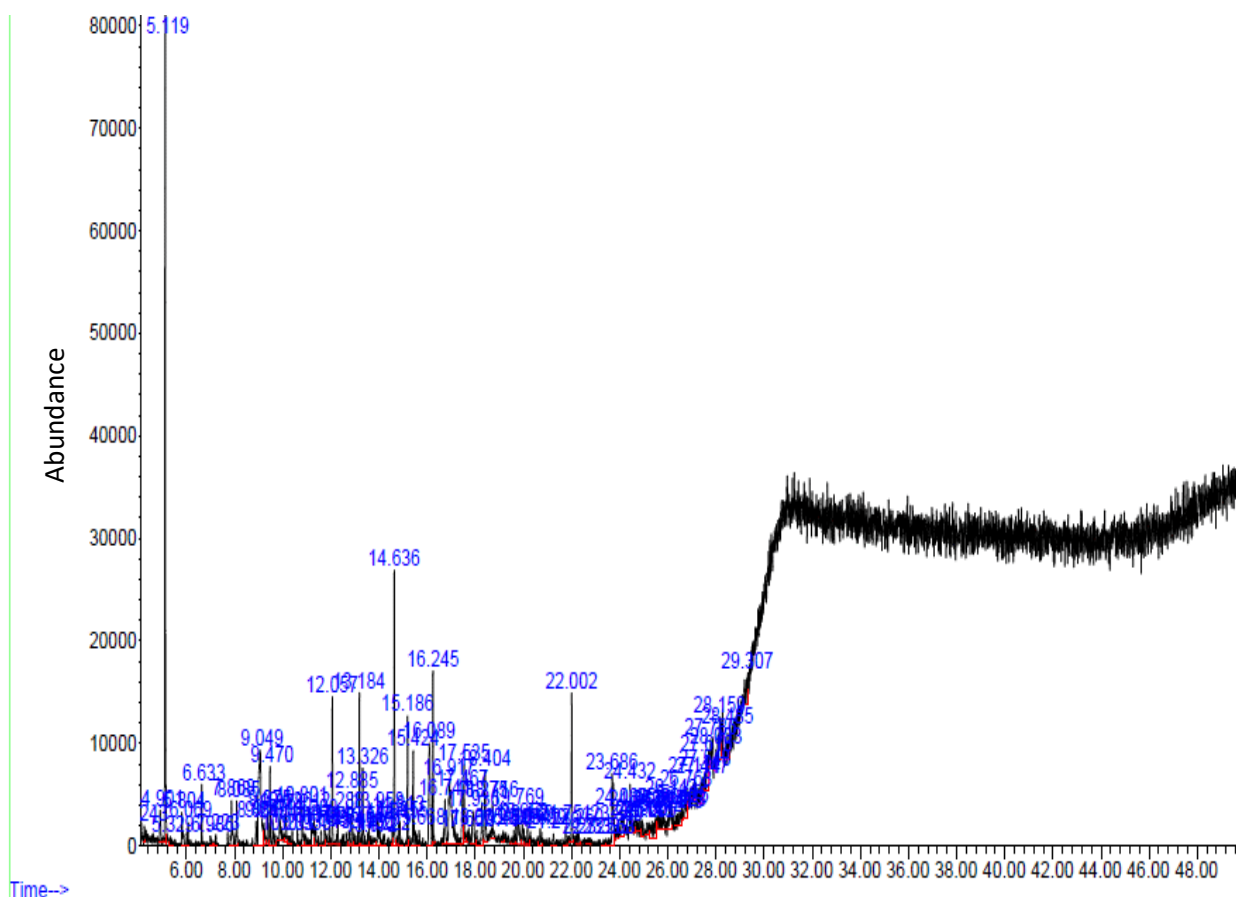


Fig. (1): GC/MS results of the fruit aqueous extract of *A. esculentus*.

Table (1): GC/MS results of biomolecules of the fruit aqueous extract of *A. esculentus*.

PK	RT	Area Percentage	Library/ID
1	4.1208	0.1644	Methanamine, N,N-difluoro-
2	4.243	0.2916	Propanal
3	4.2837	0.1567	1-Buten-3-yne
4	4.3991	0.1621	1-Buten-3-yne
5	4.6164	0.186	2,4-Pentadienenitrile
6	4.9015	0.6975	Butane, 2-methyl-
7	5.1187	15.5204	2,3-Butanediol
8	5.8044	0.7377	Pyrazine, methyl-
9	5.8722	0.2515	Dodecahydropyrido[1,2-b]isoquinolin-6-one
10	6.0148	0.2835	1H-Imidazole, 2,4-dimethyl-
11	6.0691	0.3533	Acetaldehyde, O-ethylxime-
12	6.6326	0.8905	1,3-Butadiene-1-carboxylic acid
13	6.9856	0.2091	Hydrazine, (2-methyl-1-propenyl)-
14	7.2232	0.2561	Formamide, N-(1-cyanoethenyl)
15	7.712	0.2024	Benzaldehyde, 2,4-dimethyl-
16	7.8681	0.648	Butyrolactone
17	8.0853	0.8832	Cyclopentanone, 2-methyl-

18	8.8864	0.3976	Pyridine, 3-methyl-, 1-oxide
19	9.0493	7.5124	Methanamine, N-methoxy-
20	9.219	0.4329	Methanamine, N-methoxy-
21	9.3752	0.759	o-Isopropylhydroxylamine
22	9.4702	1.3562	2-Pentenal, (E)-
23	9.5788	0.4352	1,2-Butadiene
24	9.6807	0.2122	Cyanamide, di-2-propenyl-
25	9.7893	0.2165	Methanol, (4-amino-1,2,5-oxadiazol-3-yl)(imino)-
26	9.8775	0.7559	Ethane, diazo-
27	9.959	0.1657	2-Hexen-4-yne, (E)-
28	10.1355	0.6243	Methanamine, N,N-dimethyl-, N-oxide
29	10.3935	0.2788	Benzeneacetaldehyde
30	10.6107	0.3539	Ether, heptyl hexyl
31	10.8008	0.9681	Phosphoramidous difluoride
32	11.2081	0.7214	(2H)Pyrrole-2-carbonitrile, 5-amino-3,4-dihydro-
33	11.2964	0.3335	(+)-4-Amino-4,5-dihydro-2(3H)-furanone
34	11.371	0.3938	Methyl 2-furoate
35	11.5883	0.2718	Toluene
36	11.7444	0.6746	4,4-Dimethyl-2-oxazoline
37	11.8327	0.2104	1H-Tetrazol-5-amine
38	11.9277	0.2708	Aziridine, 2-methyl-
39	12.0567	2.064	4H-Pyran-4-one, 2,3-dihydro-3,5-dihydroxy-6-methyl-
40	12.24	0.1748	S-Methyl 2-propenethioate
41	12.2875	0.5849	N-[5-(Trifluoromethyl)-1,3,4-thiadiazol-2-yl]benzamide
42	12.6337	0.2269	Quinuclidine
43	12.7491	0.2266	Isothiazole
44	12.7831	0.2634	2-Propen-1-amine, 2-bromo-N-methyl-
45	12.8849	1.0816	2-Propanone, 1-(N-cyanomethylimino-)
46	13.1157	0.2284	3-Hexenoic acid, (E)-
47	13.1836	2.144	4-Vinylphenol
48	13.3262	1.5323	5-Hydroxymethylfurfural
49	13.5366	0.2438	L-Alanine, methyl ester
50	13.5841	0.3082	DL-Gabaculine
51	13.9575	0.8232	Hydroquinone
52	14.5617	0.5327	Pentanoic acid, 4-methyl-
53	14.6364	4.0701	2-Methoxy-4-vinylphenol
54	14.8129	0.3779	Chloromethyl cyanide
55	14.874	0.3416	Chloromethyl cyanide
56	14.9554	0.165	3,5-Diketo-1,6-heptadiene
57	15.1863	1.9986	1H-Pyrrole-1-propanoic acid, methyl ester
58	15.4239	2.2126	DL-Proline, 5-oxo-, methyl ester
59	15.5053	0.2784	2-(2-Methylcyclopropyl)thiophene
60	15.6683	0.2619	1,5-Hexadiyne
61	16.0891	4.7457	Lethane
62	16.2453	2.7335	4-Vinylbenzene-1,2-diol

63	16.6865	0.2481	2,6-Difluorophenol
64	16.7409	1.4064	.beta.-D-Glucopyranose, 1,6-anhydro-
65	16.9174	2.8683	1,2,4-Benzenetriol
66	17.4672	1.8505	2-Oxazolamine, 4,5-dimethyl-
67	17.5351	1.2143	Quinuclidine
68	17.5962	0.1752	2(5H)-Oxepinone, 6,7-dihydro-
69	17.6573	0.2116	3-Methylcyclopentane-1,2-dione
70	17.6913	0.1687	3,4-Dihydro-6-methyl-2H-pyran-2-one
71	17.732	0.2037	1-Butene-3-one, dimethylhydrazone
72	17.9017	1.0597	Pyrrolidine, 1-methyl-
73	18.0646	0.272	1-Naphthalenemethanamine
74	18.2751	1.175	Pyridinium, 1-ethyl-, hydroxide
75	18.4041	2.1985	Ethyl .alpha.-d-glucoopyranoside
76	18.6145	0.2251	1,3-Dichloroallene
77	18.7164	0.7048	Phenylguanidine mononitrate
78	19.3681	0.1596	Propanamide
79	19.5989	0.2404	1H-1,3-Benzimidazole, 2-(2-pyrrolidinyl)-
80	19.6871	0.3129	2-Methyl-4-hydroxybenzoxazole
81	19.7686	1.3916	Adenine
82	19.884	0.2034	Benzaldehyde, 4-methyl-, oxime, (Z)-
83	19.9519	0.5161	2-Octyn-1-ol
84	20.1691	0.3738	2,5-Dimethyl-1-propylpyrrole
85	20.6986	0.1898	Pyrido[3,2-d]pyrimidine-2,4(1H,3H)-dione, 6-methyl-
86	20.7529	0.2404	2-(p-Tolyl)ethylamine
87	21.2485	0.2909	6-Methoxycoumaran-3-one
88	21.7509	0.3115	Ethaneperoxy acid, 1-cyano-1,4,8-trimethyl-7-nonenyl ester
89	21.8731	0.1643	Propanamide
90	22.0021	2.7334	n-Hexadecanoic acid
91	22.26	0.2084	Bicyclo[3.2.1]octane-6-carboxylic acid, 2-oxo-, methyl ester, (6S)-
92	22.294	0.2761	p-Chlorophenyl allyl ether
93	23.6856	1.5741	2-Dodecanol
94	23.7332	1.4398	Cycloheptane, methyl-
95	24.0862	0.6684	(Z)6,(Z)9-Pentadecadien-1-ol
96	24.3034	0.2238	Cyclododecanol, 1-aminomethyl-
97	24.3577	0.1584	4-Cyclohexene-1,2-dicarboximide, N-butyl-, cis-
98	24.4324	0.6401	Methyl 9,10-octadecadienoate
99	24.5478	0.1719	Cyclohexane, cyclopropyl-
100	24.5885	0.202	Bicyclo[2.2.1]heptan-2-ol, 3,3-dimethyl-, exo-
101	24.6428	0.3589	Dodecahydropyrido[1,2-b]isoquinolin-6-one
102	24.7107	0.1899	Cyclohexane-1,3-dione, 2-allylaminomethylene-5,5-dimethyl-
103	24.9347	0.1819	R(-)3,7-Dimethyl-1,6-octadiene
104	24.9619	0.1808	Carbonic acid, 2,2,2-trichloroethyl cyclohexylmethyl ester

105	25.4778	0.1874	Dodecahydropyrido[1,2-b]isoquinolin-6-one
106	25.5865	0.2029	9-Borabicyclo[3.3.1]nonane, 9-[3-(dimethylamino)propyl]-
107	25.7222	0.284	Cyclohexane, 1-(cyclohexylmethyl)-4-ethyl-, cis-
108	25.8037	0.1803	Pyridine, 1,2,3,6-tetrahydro-1-methyl-4-[4-chlorophenyl]-
109	26.0141	0.4431	2-Pyridinemethanol 3,5-dichloro-4-hydroxy-6-methyl-
110	26.0617	0.2612	2H-1,3-benzoxazine-6-carboxylic acid, 3,4-dihydro-3-methyl-, methyl ester
111	26.1771	0.225	[1,2,4]Triazolo[1,5-a]pyrimidine-6-carboxylic acid, 7-amino-, ethyl ester
112	26.2042	0.161	[1,2,4]Triazolo[1,5-a]pyrimidine-6-carboxylic acid, 4,7-dihydro-7-imino-, ethyl ester
113	26.2585	0.1904	3,5-Dimethylbenzaldehyde thiocarbamoylhydrazone
114	26.3536	0.172	Dodecahydropyrido[1,2-b]isoquinolin-6-one
115	26.4011	0.1582	Hexahydropyridine, 1-methyl-4-[4,5-dihydroxyphenyl]-
116	26.5776	0.1799	5H-dibenzo[a,d]cyclohepten-5-amine
117	26.7066	0.4204	Silicic acid, diethyl bis(trimethylsilyl) ester
118	26.7677	0.2595	2-Ethylacridine
119	26.917	0.3095	1,1,1,3,5,5,5-Heptamethyltrisiloxane
120	26.9578	0.4575	1,1,1,3,5,5,5-Heptamethyltrisiloxane
121	27.1546	0.5674	Silicic acid, diethyl bis(trimethylsilyl) ester
122	27.6163	0.4293	Silicic acid, diethyl bis(trimethylsilyl) ester
123	28.4852	0.4669	7,7,9,9,11,11-Hexamethyl-3,6,8,10,12,15-hexaoxa-7,9,11-trisilaheptadecane

UV-Visible spectrophotometer

The current study found that the colour of the reaction mixture changed with time, from light green to dark brown, and that the colour transformation process required five days as shown in fig. (2) to ensure that the silver nanoparticles were generated, it was examined with a UV-vis instrument, where the highest peak was observed at 390 nm (Fig. 3). This spectrum shows that the manufactured

nanoparticles are of silver. UV-vis analysis is used to explain the colour change of the solution in order to understand the production of nanoparticles, and it is caused by the phenomenon of plasmon absorption, which arises from the absorption of electrons on the surface of AgNPs. If the maximum absorption peak of this study is about 400 nm, it verifies that the nanoparticles' chemical composition is silver (Praba *et al.*, 2015).



Fig. (2): The change in colour of the reaction solution indicates the manufacturing of silver nanoparticles using *A. esculentus* fruit aqueous extract.

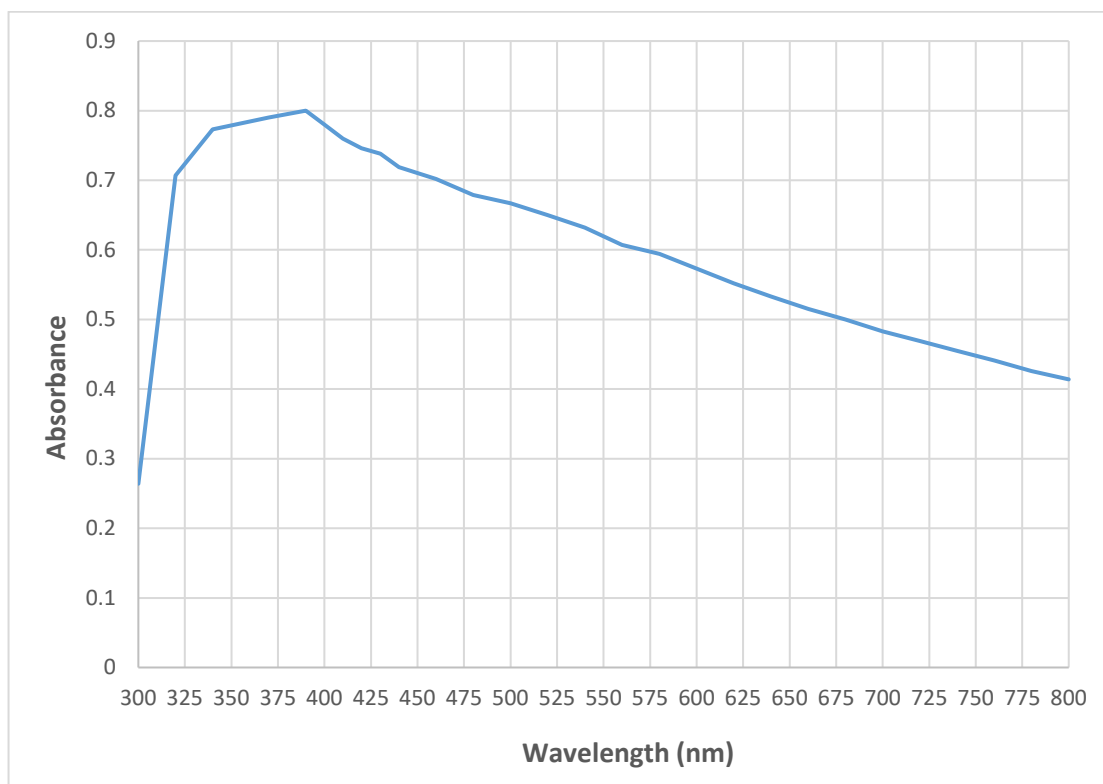


Fig. (3): UV-vis characterization of the absorbance peaks of silver nanoparticles produced by *A. esculentus* fruit aqueous extract.

Fourier Transform Infrared Spectroscopy (FTIR)

The results of the FTIR for the aqueous extract of *A. esculentus* plant and the nanoparticles recorded the presence of the O-H group, which indicates the presence of an alcohol compound or phenol, then the N-H groups, which refer to amino acids or alkaloids. It was also observed that there was a creep in the readings of this analysis when comparing the results of the aqueous extract. With the results of nanoparticles as in packages 3385 to 3384, 2958 to 2924, 1643 to 1627, 1556 to 1531, 1411 to 1446, and 1246 to 1240 cm^{-1} , this change in values indicates the formation of

nanoparticles Table 2 Fig 4 and 5. The active groups found in the plant extract that contributed to the reduction and stabilization of silver nitrate to silver nanoparticles were identified using FTIR analysis (Praba *et al.*, 2015). The current study recorded the presence of alcohols, carbohydrates, amines, and amino acid residues in the *A. esculentus* fruit aqueous extract and according to Moteriya *et al.* (2017), these compounds are involved in the synthesis of AgNPs.

Table (2): FTIR results of *A. esculentus* aqueous extract and AgNPs.

FTIR of AgNPs			FTIR of aqueous extract		
Compound class	Group	Absorption(cm^{-1})	Compound class	Group	Absorption(cm^{-1})
alcohol	O-H	3415	alcohol	O-H	3415
amine	N-H	3384	amine	N-H	3385
aromatic	C-H	3086	aliphatic	C-H	2958
aliphatic	C-H	2924	aliphatic	C-H	2927
Primary amine	N-H	1627	Primary amine	N-H	1643
Aromatic ring	C=C	1531	Aromatic ring	C=C	1556
Alkane (methylene group)	C-H	1446	Methyl group	C-H	1411
alkane (methyl group)	C-H	1396	amine	C-N	1246
amine	C-N	1240			

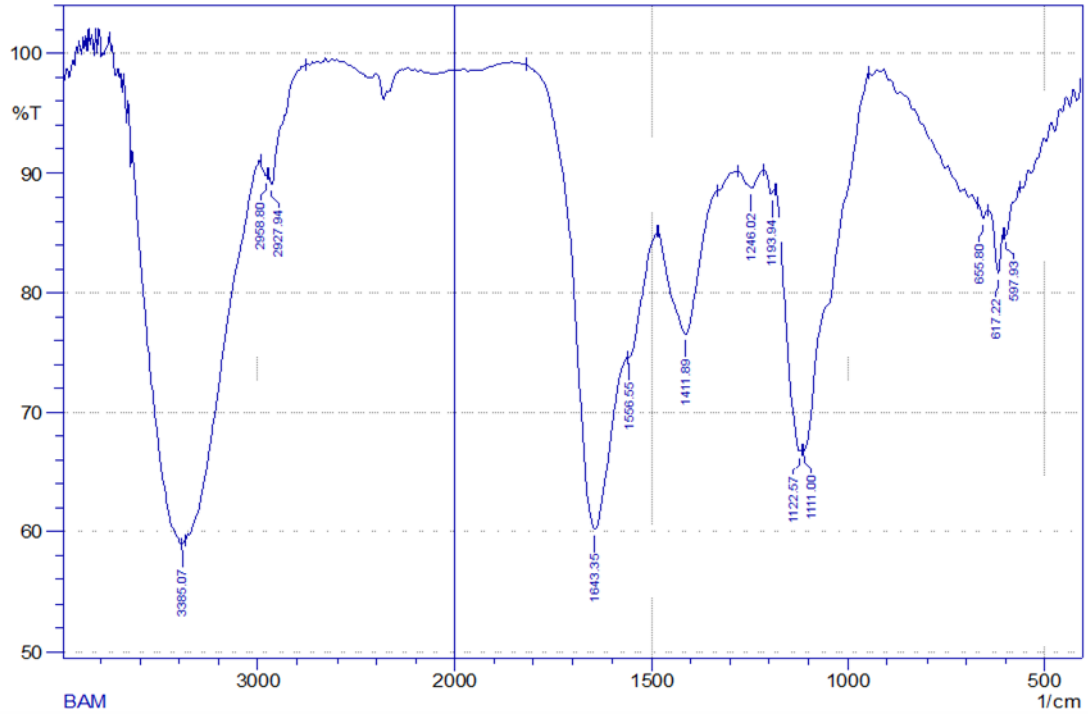


Fig. (4): FTIR results of *A. esculentus* fruit aqueous extract.

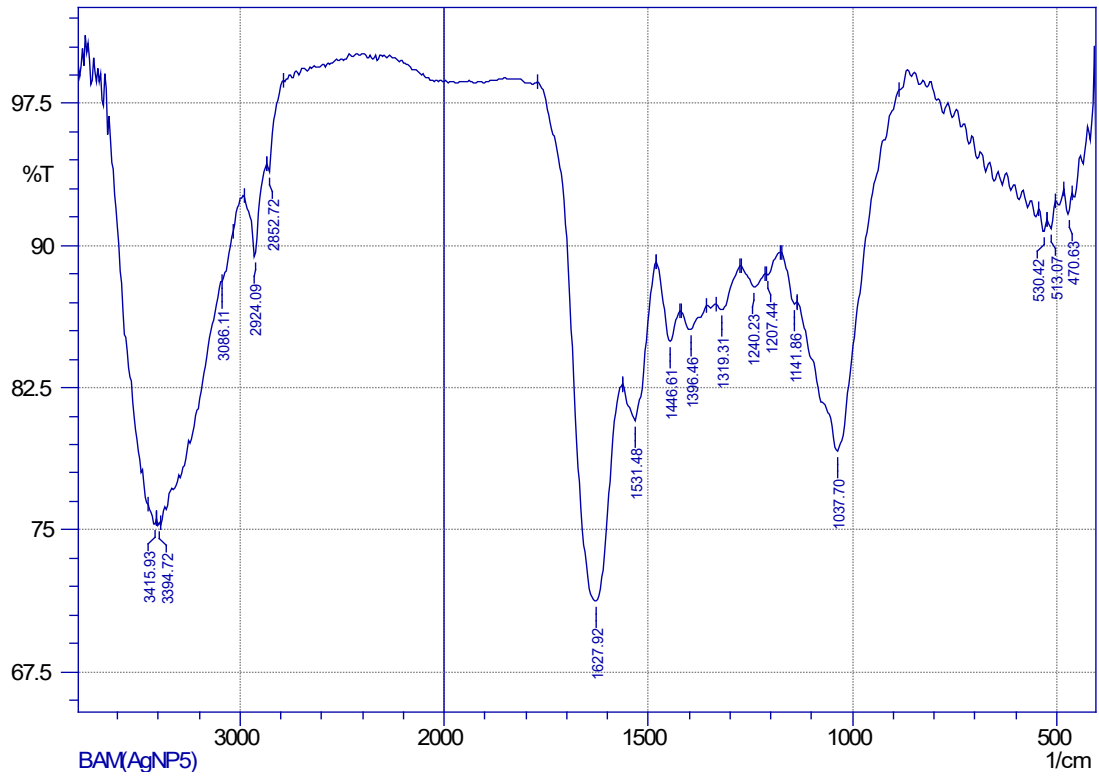


Fig. (5): FTIR results of AgNPs using *A. esculentus* fruit aqueous extract.

X-Ray Diffraction Analysis (XRD)

As shown in fig. (6), the XRD analysis revealed the presence of six diffraction peaks at 2θ of 27.2343, 31.5615, 45.3002, 56.8269, 63.1514, and 74.5365 which correspond to the levels of silver crystals (111, 200, 220, 222, 410, and 420 respectively). These XRD peaks represent face-centered cubic,

and the sharpness of the peaks verifies that the created particles are Nano size (Fig. 6). These strong peaks also corroborate the effectiveness of Bragg's reflection, which reveals the silver cubic form centered on the face (Alaqad & Saleh, 2016).

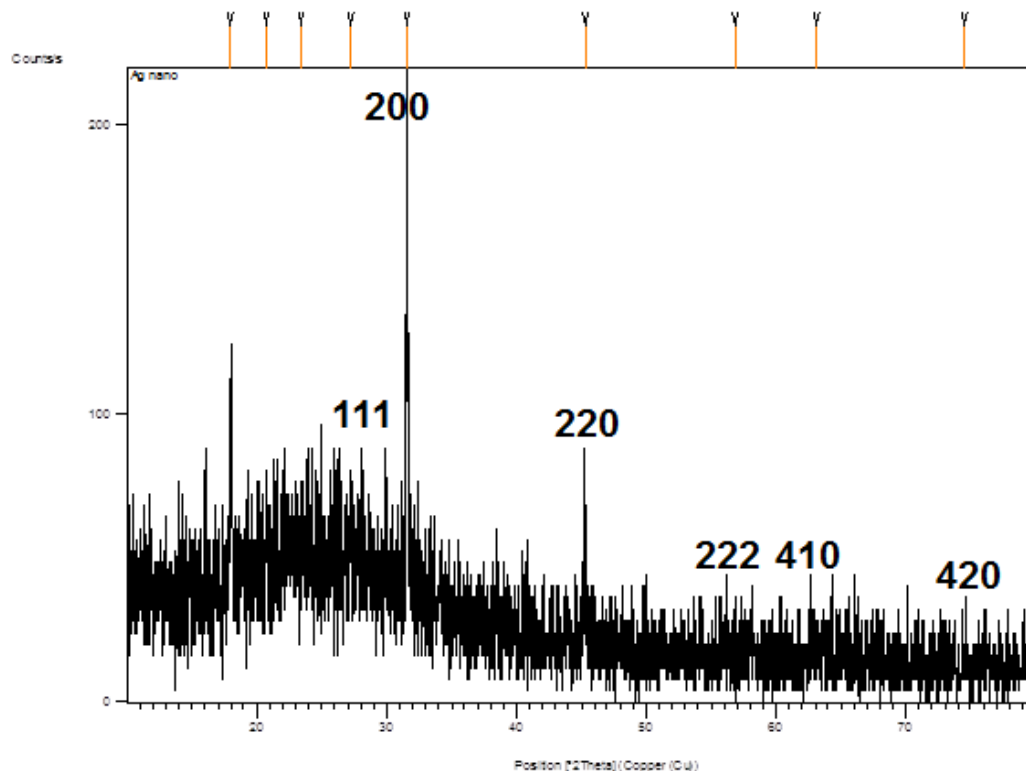


Fig. (6): XRD diffraction pattern results of silver nanoparticles composed by *A. esculentus* fruit aqueous extract.

Scanning Electron Microscope (SEM)

The results of SEM showed that the nanoparticles manufactured in the current study had spherical to semi-spherical shapes, with sizes ranging from 21.66 to 57.67 nm

(Fig. 7). Scanning electron microscopes (SEM) are used to determine the shapes and sizes of produced silver nanoparticles, and electrons are employed to magnify the studied objects instead of light in compound microscopes (Balavijayalakshmi & Ramalakshmi, 2017).

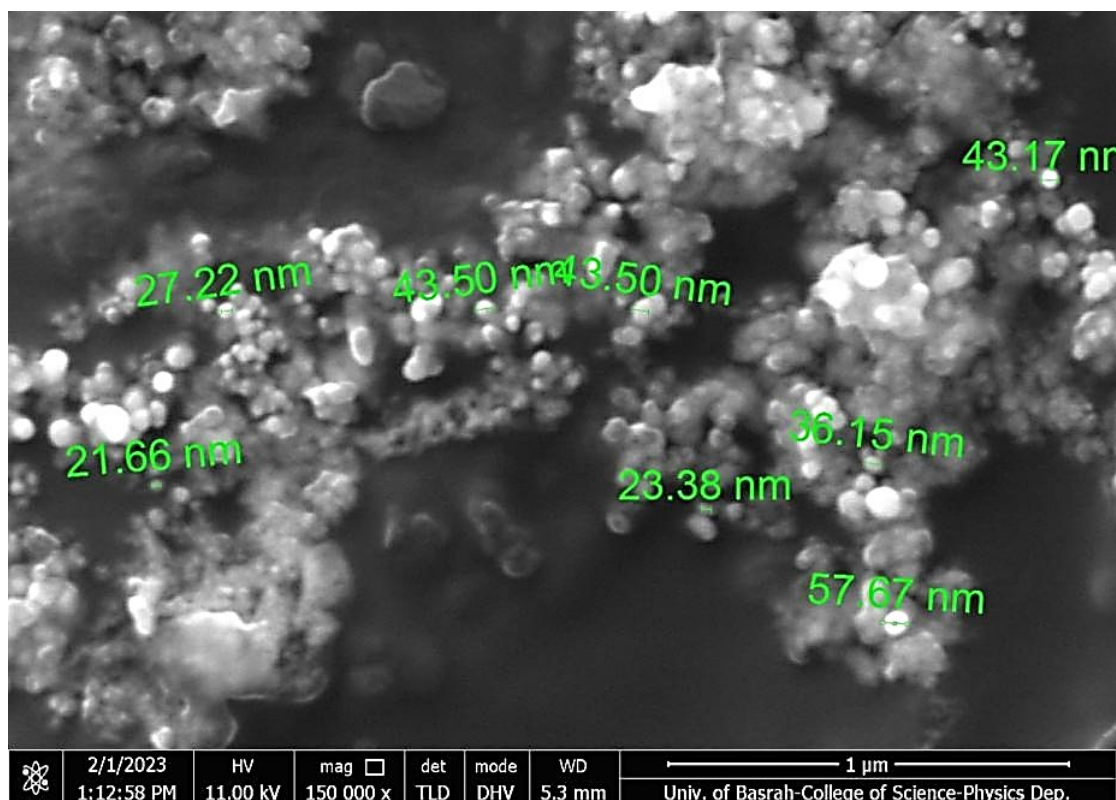


Fig. (7): SEM image of silver nanoparticles composed by *A. esculentus* fruit aqueous extract.

Energy-Dispersive X-Ray Spectroscopy (EDX)

X-ray energy dispersive spectroscopy (EDX) research was performed to validate the creation of silver nanoparticles. Silver EDS peaks demonstrate the existence of silver as a component element, as well as the production and purity of silver nanoparticles generated from leaf and callus extracts (Fig. 8). The existence of silver nanoparticles was confirmed by the occurrence of a strong peak in the silver region at 3 keV owing to Surface Plasmon Resonance. Due to Surface Plasmon Resonance, silver nanocrystals often exhibit an optical absorption peak of about 3 keV. The elemental analysis of the produced silver

nanoparticles revealed that silver was the most abundant element, followed by chlorine, sulfur, and phosphorus. The low oxygen signal could be due to X-ray emission from carbohydrates/proteins/enzymes in the extracts, or it could be due to the formation of silver oxide nanoparticles after the synthesis of silver nanoparticles, which react with water in the solution because the nanoparticles are highly reactive due to their high surface to volume ratio (Jamel *et al.*, 2017). This technique is based on the impact of electrons with nanoparticles, which produces a unique spectrum of X-rays for each element. The chemical composition of the nanoparticles component is known in this analysis (Akintelu *et al.*, 2020).

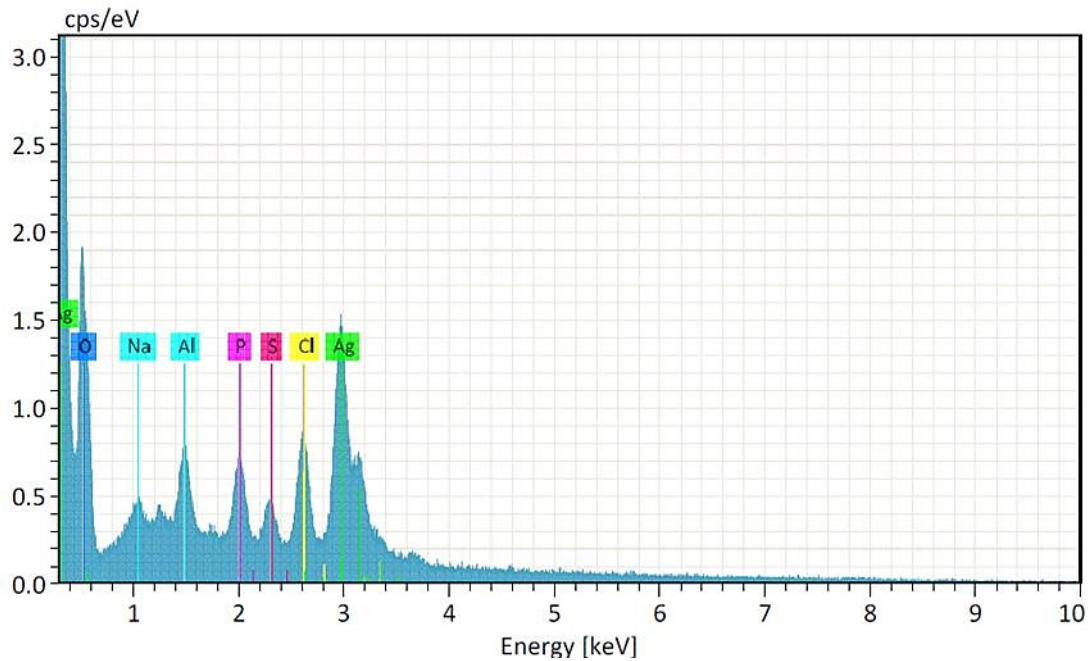


Fig. (8): EDX spectrum analysis results of silver nanoparticles composed by *A. esculentus* fruit aqueous extract.

Identification of bacteria

Bacteria were identified in the current study based on morphological characteristics and biochemical and molecular tests using the diagnostic 16SrRNA gene. After obtaining the DNA sequences from Macrogen Company

(Korea), these sequences were used for identification of the bacteria based on the information base in the NCBI blast gene bank after alignment it with the reference strains and recording the presence of four species and it: *Alcaligenes faecalis* (2R), *Escherichia coli* (3R), *Staphylococcus auricularis* (8F), and, *Escherichia coli* (11F) (Figs. 9-16).

OQ160687.1:27-829	GCTTGCTCTCTTGGCGGCAGTGGCGGACGGGTGAGTAATATATCGGAACGTGCCAGTA	60
OQ160686.1:37-839	GCTTGCTCTCTTGGCGGCAGTGGCGGACGGGTGAGTAATATATCGGAACGTGCCAGTA	60
OQ363280.1:21-823	GCTTGCTCTCTTGGCGGCAGTGGCGGACGGGTGAGTAATATATCGGAACGTGCCAGTA	60
2R(this	GCTTGCTCTCTTGGCGGCAGTGGCGGACGGGTGAGTAATATATCGGAACGTGCCAGTA	60
KX302624.1:57-859	GCTTGCTCTCTTGGCGGCAGTGGCGGACGGGTGAGTAATATATCGGAACGTGCCAGTA	60
KX828579.1:15-817	GCTTGCTCTCTTGGCGGCAGTGGCGGACGGGTGAGTAATATATCGGAACGTGCCAGTA	60
KX828569.1:17-819	GCTTGCTCTCTTGGCGGCAGTGGCGGACGGGTGAGTAATATATCGGAACGTGCCAGTA	60
KX462790.1:39-841	GCTTGCTCTCTTGGCGGCAGTGGCGGACGGGTGAGTAATATATCGGAACGTGCCAGTA	60
AB847929.1:38-840	GCTTGCTCTCTTGGCGGCAGTGGCGGACGGGTGAGTAATATATCGGAACGTGCCAGTA	60
GQ383898.1:28-830	GCTTGCTCTCTTGGCGGCAGTGGCGGACGGGTGAGTAATATATCGGAACGTGCCAGTA	60
OM293496.1:19-821	GCTTGCTCTCTTGGCGGCAGTGGCGGACGGGTGAGTAATATATCGGAACGTGCCAGTA	60

OQ160687.1:27-829	GCGGGGGATAACTACTCGAAAAGAGTGGCTAATACCGCATAACGCCCTACGGGGGAAAAGGGG	120
OQ160686.1:37-839	GCGGGGGATAACTACTCGAAAAGAGTGGCTAATACCGCATAACGCCCTACGGGGGAAAAGGGG	120
OQ363280.1:21-823	GCGGGGGATAACTACTCGAAAAGAGTGGCTAATACCGCATAACGCCCTACGGGGGAAAAGGGG	120
2R(this	GCGGGGGATAACTACTCGAAAAGAGTGGCTAATACCGCATAACGCCCTACGGGGGAAAAGGGG	120
KX302624.1:57-859	GCGGGGGATAACTACTCGAAAAGAGTGGCTAATACCGCATAACGCCCTACGGGGGAAAAGGGG	120
KX828579.1:15-817	GCGGGGGATAACTACTCGAAAAGAGTGGCTAATACCGCATAACGCCCTACGGGGGAAAAGGGG	120
KX828569.1:17-819	GCGGGGGATAACTACTCGAAAAGAGTGGCTAATACCGCATAACGCCCTACGGGGGAAAAGGGG	120
KX462790.1:39-841	GCGGGGGATAACTACTCGAAAAGAGTGGCTAATACCGCATAACGCCCTACGGGGGAAAAGGGG	120
AB847929.1:38-840	GCGGGGGATAACTACTCGAAAAGAGTGGCTAATACCGCATAACGCCCTACGGGGGAAAAGGGG	120
GQ383898.1:28-830	GCGGGGGATAACTACTCGAAAAGAGTGGCTAATACCGCATAACGCCCTACGGGGGAAAAGGGG	120
OM293496.1:19-821	GCGGGGGATAACTACTCGAAAAGAGTGGCTAATACCGCATAACGCCCTACGGGGGAAAAGGGG	120

OQ160687.1:27-829	GGGATCGCAAGACCTCTCACTATTGGAGCGGCCGATATCGGATTAGCTAGTTGGTGGGGT	180
OQ160686.1:37-839	GGGATCGCAAGACCTCTCACTATTGGAGCGGCCGATATCGGATTAGCTAGTTGGTGGGGT	180
OQ363280.1:21-823	GGGATCGCAAGACCTCTCACTATTGGAGCGGCCGATATCGGATTAGCTAGTTGGTGGGGT	180
2R(this	GGGATCGCAAGACCTCTCACTATTGGAGCGGCCGATATCGGATTAGCTAGTTGGTGGGGT	180
KX302624.1:57-859	GGGATCGCAAGACCTCTCACTATTGGAGCGGCCGATATCGGATTAGCTAGTTGGTGGGGT	180
KX828579.1:15-817	GGGATCGCAAGACCTCTCACTATTGGAGCGGCCGATATCGGATTAGCTAGTTGGTGGGGT	180
KX828569.1:17-819	GGGATCGCAAGACCTCTCACTATTGGAGCGGCCGATATCGGATTAGCTAGTTGGTGGGGT	180
KX462790.1:39-841	GGGATCGCAAGACCTCTCACTATTGGAGCGGCCGATATCGGATTAGCTAGTTGGTGGGGT	180
AB847929.1:38-840	GGGATCGCAAGACCTCTCACTATTGGAGCGGCCGATATCGGATTAGCTAGTTGGTGGGGT	180
GQ383898.1:28-830	GGGATCGCAAGACCTCTCACTATTGGAGCGGCCGATATCGGATTAGCTAGTTGGTGGGGT	180
OM293496.1:19-821	GGGATCGCAAGACCTCTCACTATTGGAGCGGCCGATATCGGATTAGCTAGTTGGTGGGGT	180

Fig. (9): Multiple sequence alignment analysis of *Alcaligenes faecalis* (2R).

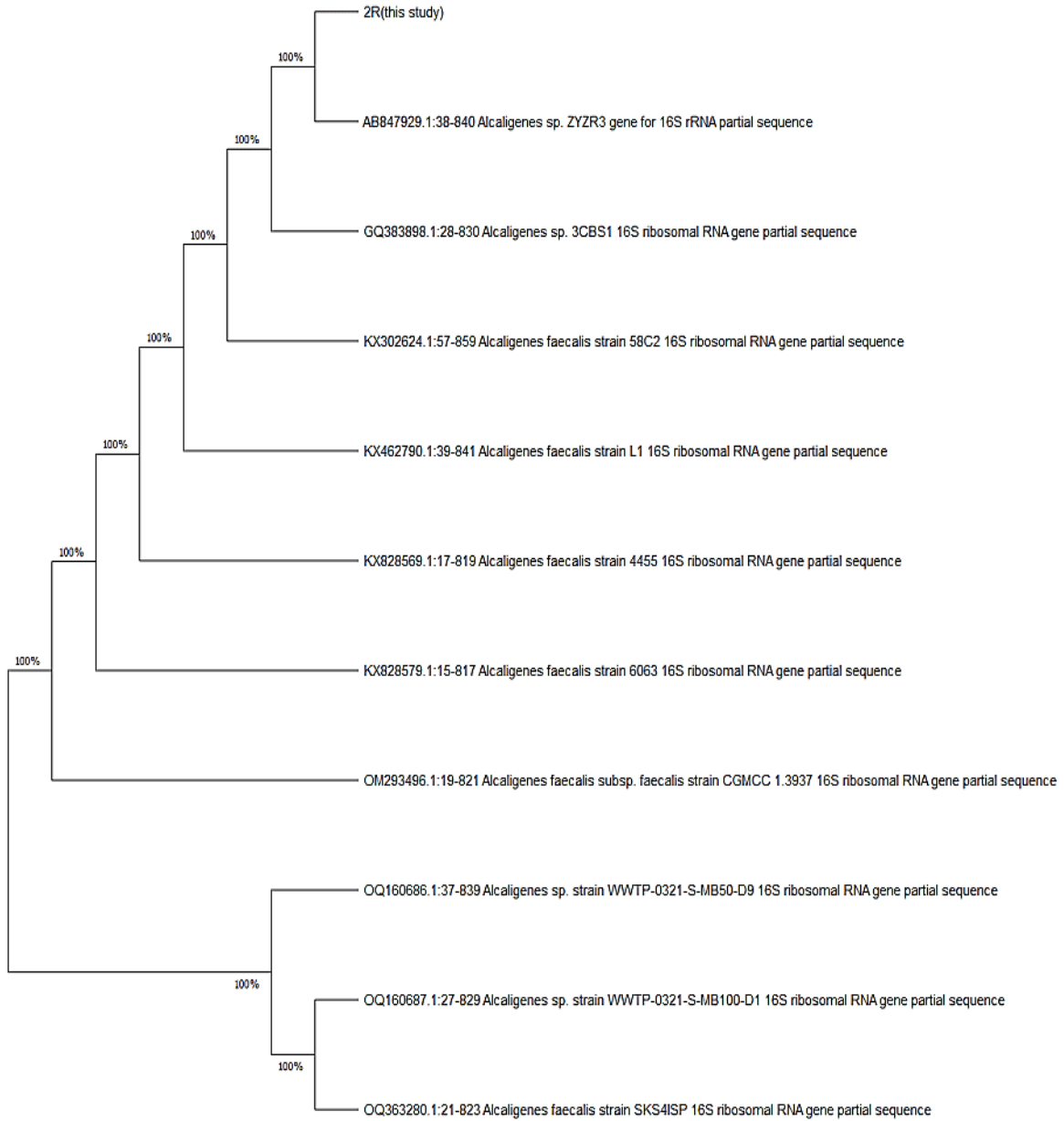


Fig. (10): Phylogenetic tree of *Alcaligenes faecalis* (2R).

KU612261.1:1-805	AGCTTGCTGCTTYGCTGACGAGTGGCGGACGGGTGAGTAATGTCTGGGAAACTGCCTGAT	60
OP218938.1:44-848	AGCTTGCTGCTTYGCTGACGAGTGGCGGACGGGTGAGTAATGTCTGGGAAACTGCCTGAT	60
MK713895.1:35-839	AGCTTGCTGCTTCGCTGACGAGTGGCGGACGGGTGAGTAATGTCTGGGAAACTGCCTGAT	60
MK878418.1:200-1004	AGCTTGCTGCTTCGCTGACGAGTGGCGGACGGGTGAGTAATGTCTGGGAAACTGCCTGAT	60
KX602657.1:52-856	AGCTTGCTGCTTCGCTGACGAGTGGCGGACGGGTGAGTAATGTCTGGGAAACTGCCTGAT	60
MW832248.1:31-835	AGCTTGCTGCTTCGCTGACGAGTGGCGGACGGGTGAGTAATGTCTGGGAAACTGCCTGAT	60
3(this	AGCTTGCTGCTTCGCTGACGAGTGGCGGACGGGTGAGTAATGTCTGGGAAACTGCCTGAT	60

KU612261.1:1-805	GGAGGGGGATAAATACTGGAACCGGTAGCTAATACCGCATAACGTGCGCAAGACCAAAGAG	120
OP218938.1:44-848	GGAGGGGGATAAATACTGGAACCGGTAGCTAATACCGCATAACGTGCGCAAGACCAAAGAG	120
MK713895.1:35-839	GGAGGGGGATAAATACTGGAACCGGTAGCTAATACCGCATAACGTGCGCAAGACCAAAGAG	120
MK878418.1:200-1004	GGAGGGGGATAAATACTGGAACCGGTAGCTAATACCGCATAACGTGCGCAAGACCAAAGAG	120
KX602657.1:52-856	GGAGGGGGATAAATACTGGAACCGGTAGCTAATACCGCATAACGTGCGCAAGACCAAAGAG	120
MW832248.1:31-835	GGAGGGGGATAAATACTGGAACCGGTAGCTAATACCGCATAACGTGCGCAAGACCAAAGAG	120
3(this	GGAGGGGGATAAATACTGGAACCGGTAGCTAATACCGCATAACGTGCGCAAGACCAAAGAG	120

KU612261.1:1-805	GGGGACCTTCGGGCCTCTTGCCATCGGATGTGCCAGATGGGATTAGCTTGTAGGTGGGG	180
OP218938.1:44-848	GGGGACCTTCGGGCCTCTTGCCATCGGATGTGCCAGATGGGATTAGCTTGTAGGTGGGG	180
MK713895.1:35-839	GGGGACCTTCGGGCCTCTTGCCATCGGATGTGCCAGATGGGATTAGCTTGTAGGTGGGG	180
MK878418.1:200-1004	GGGGACCTTCGGGCCTCTTGCCATCGGATGTGCCAGATGGGATTAGCTTGTAGGTGGGG	180
KX602657.1:52-856	GGGGACCTTCGGGCCTCTTGCCATCGGATGTGCCAGATGGGATTAGCTTGTAGGTGGGG	180
MW832248.1:31-835	GGGGACCTTCGGGCCTCTTGCCATCGGATGTGCCAGATGGGATTAGCTTGTAGGTGGGG	180
3(this	GGGGACCTTCGGGCCTCTTGCCATCGGATGTGCCAGATGGGATTAGCTTGTAGGTGGGG	180

KU612261.1:1-805	TAACGGCTCACCTAGGCGACGATCCCTAGCTGGTCTGAGAGGATGACCAGCCACACTGGA	240
OP218938.1:44-848	TAACGGCTCACCTAGGCGACGATCCCTAGCTGGTCTGAGAGGATGACCAGCCACACTGGA	240
MK713895.1:35-839	TAACGGCTCACCTAGGCGACGATCCCTAGCTGGTCTGAGAGGATGACCAGCCACACTGGA	240
MK878418.1:200-1004	TAACGGCTCACCTAGGCGACGATCCCTAGCTGGTCTGAGAGGATGACCAGCCACACTGGA	240
KX602657.1:52-856	TAACGGCTCACCTAGGCGACGATCCCTAGCTGGTCTGAGAGGATGACCAGCCACACTGGA	240
MW832248.1:31-835	TAACGGCTCACCTAGGCGACGATCCCTAGCTGGTCTGAGAGGATGACCAGCCACACTGGA	240
3(this	TAACGGCTCACCTAGGCGACGATCCCTAGCTGGTCTGAGAGGATGACCAGCCACACTGGA	240

Fig. (11): Multiple sequence alignment analysis of *Escherichia coli* (3R).

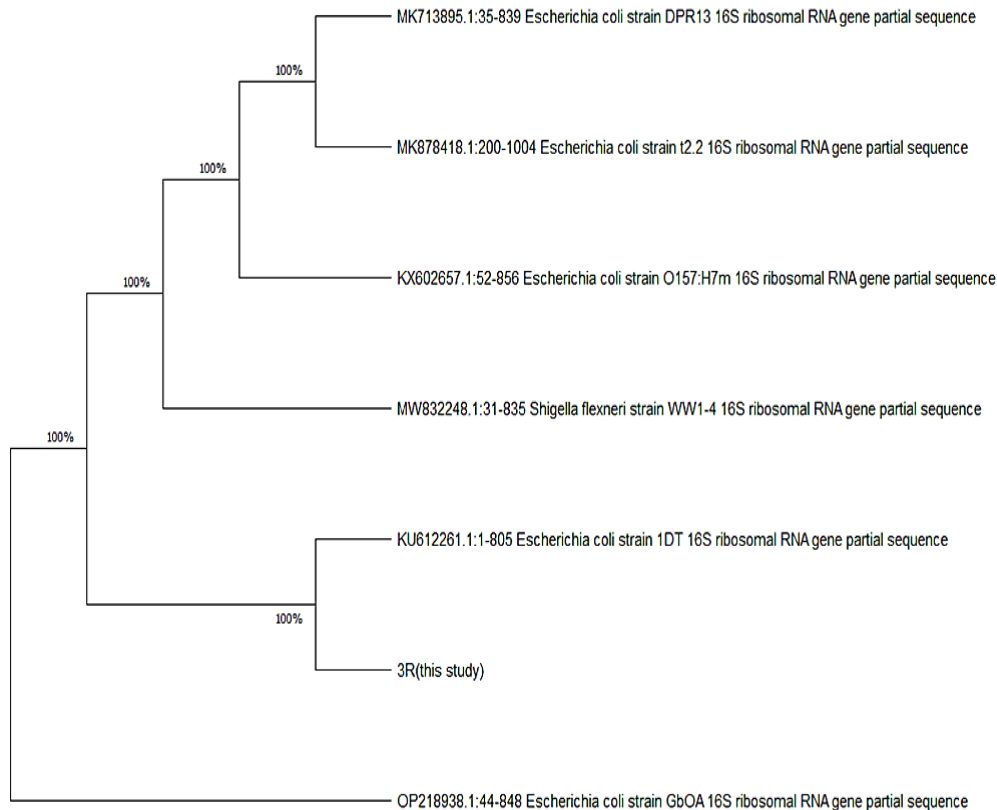


Fig. (12): Phylogenetic tree of *Escherichia coli* (3R).


```

MK093899.1:34-526      AGTCGAGCGAACAGATAAGGAGCTTGCTCCTTTGACGTTAGCGGCGGACGGGTGAGTAAC  60
MF678866.1:33-525      AGTCGAGCGAACAGATAAGGAGCTTGCTCCTTTGACGTTAGCGGCGGACGGGTGAGTAAC  60
CP065712.1:303348-303840  AGTCGAGCGAACAGATAAGGAGCTTGCTCCTTTGACGTTAGCGGCGGACGGGTGAGTAAC  60
CP065712.1:347488-347980  AGTCGAGCGAACAGATAAGGAGCTTGCTCCTTTGACGTTAGCGGCGGACGGGTGAGTAAC  60
CP065712.1:861630-862122  AGTCGAGCGAACAGATAAGGAGCTTGCTCCTTTGACGTTAGCGGCGGACGGGTGAGTAAC  60
8F(this study)         AGTCGAGCGAACAGATAAGGAGCTTGCTCCTTTGACGTTAGCGGCGGACGGGTGAGTAAC  60
MF678922.1:5-497       AGTCGAGCGAACAGATAAGGAGCTTGCTCCTTTGACGTTAGCGGCGGACGGGTGAGTAAC  60
LC383924.1:33-525      AGTCGAGCGAACAGATAAGGAGCTTGCTCCTTTGACGTTAGCGGCGGACGGGTGAGTAAC  60
MG561811.1:3-495       AGTCGAGCGAACAGATAAGGAGCTTGCTCCTTTGACGTTAGCGGCGGACGGGTGAGTAAC  60
CP065712.1:745146-745638  AGTCGAGCGAACAGATAAGGAGCTTGCTCCTTTGACGTTAGCGGCGGACGGGTGAGTAAC  60
CP065712.1:654018-654510  AGTCGAGCGAACAGATAAGGAGCTTGCTCCTTTGACGTTAGCGGCGGACGGGTGAGTAAC  60
*****

MK093899.1:34-526      ACGTGGGTAACCTACCTATAAGACTGGAATAACTCCGGGAACCGGGGCTAATGCCGGAT  120
MF678866.1:33-525      ACGTGGGTAACCTACCTATAAGACTGGAATAACTCCGGGAACCGGGGCTAATGCCGGAT  120
CP065712.1:303348-303840  ACGTGGGTAACCTACCTATAAGACTGGAATAACTCCGGGAACCGGGGCTAATGCCGGAT  120
CP065712.1:347488-347980  ACGTGGGTAACCTACCTATAAGACTGGAATAACTCCGGGAACCGGGGCTAATGCCGGAT  120
CP065712.1:861630-862122  ACGTGGGTAACCTACCTATAAGACTGGAATAACTCCGGGAACCGGGGCTAATGCCGGAT  120
8F(this study)         ACGTGGGTAACCTACCTATAAGACTGGAATAACTCCGGGAACCGGGGCTAATGCCGGAT  120
MF678922.1:5-497       ACGTGGGTAACCTACCTATAAGACTGGAATAACTCCGGGAACCGGGGCTAATGCCGGAT  120
LC383924.1:33-525      ACGTGGGTAACCTACCTATAAGACTGGAATAACTCCGGGAACCGGGGCTAATGCCGGAT  120
MG561811.1:3-495       ACGTGGGTAACCTACCTATAAGACTGGAATAACTCCGGGAACCGGGGCTAATGCCGGAT  120
CP065712.1:745146-745638  ACGTGGGTAACCTACCTATAAGACTGGAATAACTCCGGGAACCGGGGCTAATGCCGGAT  120
CP065712.1:654018-654510  ACGTGGGTAACCTACCTATAAGACTGGAATAACTCCGGGAACCGGGGCTAATGCCGGAT  120
*****

MK093899.1:34-526      AACATGTTGAACCGCATGGTTCTACAGTCAAAGGCGGCTTTGCTGTCACCTTATAGATGGA  180
MF678866.1:33-525      AACATGTTGAACCGCATGGTTCTACAGTCAAAGGCGGCTTTGCTGTCACCTTATAGATGGA  180
CP065712.1:303348-303840  AACATGTTGAACCGCATGGTTCTACAGTCAAAGGCGGCTTTGCTGTCACCTTATAGATGGA  180
CP065712.1:347488-347980  AACATGTTGAACCGCATGGTTCTACAGTCAAAGGCGGCTTTGCTGTCACCTTATAGATGGA  180
CP065712.1:861630-862122  AACATGTTGAACCGCATGGTTCTACAGTCAAAGGCGGCTTTGCTGTCACCTTATAGATGGA  180
8F(this study)         AACATGTTGAACCGCATGGTTCTACAGTCAAAGGCGGCTTTGCTGTCACCTTATAGATGGA  180
MF678922.1:5-497       AACATGTTGAACCGCATGGTTCTACAGTCAAAGGCGGCTTTGCTGTCACCTTATAGATGGA  180

```

Fig. (13): Multiple sequence alignment analysis of *Staphylococcus auricularis* (8F).

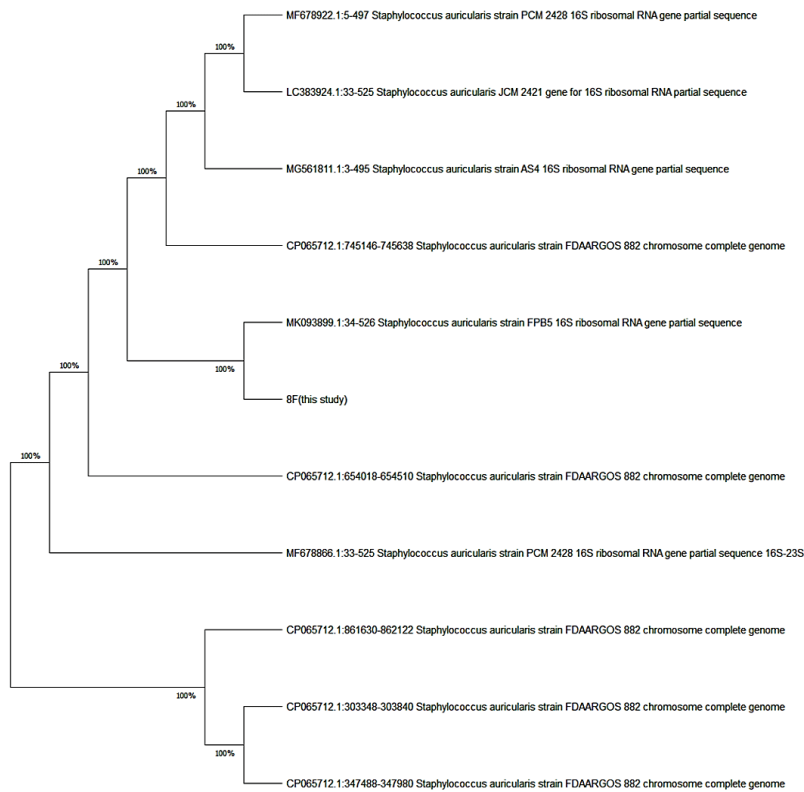


Fig. (14): Phylogenetic tree of *Staphylococcus auricularis* (8F).

```

11F(this
KY780352.1:52-469      TTGCTGACGAGTGGCCGACGGGTGAGTAATGTCTGGGAAACTGCCTGATGGAGGGGGATA 60
ON054402.1:45-462      TTGCTGACGAGTGGCCGACGGGTGAGTAATGTCTGGGAAACTGCCTGATGGAGGGGGATA 60
MT573069.1:23-440      TTGCTGACGAGTGGCCGACGGGTGAGTAATGTCTGGGAAACTGCCTGATGGAGGGGGATA 60
MT516163.1:34-451      TTGCTGACGAGTGGCCGACGGGTGAGTAATGTCTGGGAAACTGCCTGATGGAGGGGGATA 60
MT114948.1:4-421       TTGCTGACGAGTGGCCGACGGGTGAGTAATGTCTGGGAAACTGCCTGATGGAGGGGGATA 60
MN147831.1:22-438      TTGCTGACGAGTGGCCGACGGGTGAGTAATGTCTGGGAAACTGCCTGATGGAGGGGGATA 60
MN121585.1:27-443      TTGCTGACGAGTGGCCGACGGGTGAGTAATGTCTGGGAAACTGCCTGATGGAGGGGGATA 60
MN121155.1:27-444      TTGCTGACGAGTGGCCGACGGGTGAGTAATGTCTGGGAAACTGCCTGATGGAGGGGGATA 60
MH725718.1:35-443      TTGCTGACGAGTGGCCGACGGGTGAGTAATGTCTGGGAAACTGCCTGATGGAGGGGGATA 60
MH725704.1:35-443      TTGCTGACGAGTGGCCGACGGGTGAGTAATGTCTGGGAAACTGCCTGATGGAGGGGGATA 60
MH725703.1:35-443      TTGCTGACGAGTGGCCGACGGGTGAGTAATGTCTGGGAAACTGCCTGATGGAGGGGGATA 60
*****

11F(this
KY780352.1:52-469      ACTACTGGAAACGGTAGCTAATACCGCATAACGTCGCAAGACCAAGAGGGGGACCTTCG 120
ON054402.1:45-462      ACTACTGGAAACGGTAGCTAATACCGCATAACGTCGCAAGACCAAGAGGGGGACCTTCG 120
MT573069.1:23-440      ACTACTGGAAACGGTAGCTAATACCGCATAACGTCGCAAGACCAAGAGGGGGACCTTCG 120
MT516163.1:34-451      ACTACTGGAAACGGTAGCTAATACCGCATAACGTCGCAAGACCAAGAGGGGGACCTTCG 120
MT114948.1:4-421       ACTACTGGAAACGGTAGCTAATACCGCATAACGTCGCAAGACCAAGAGGGGGACCTTCG 120
MN147831.1:22-438      ACTACTGGAAACGGTAGCTAATACCGCATAACGTCGCAAGACCAAGAGGGGGACCTTCG 120
MN121585.1:27-443      ACTACTGGAAACGGTAGCTAATACCGCATAACGTCGCAAGACCAAGAGGGGGACCTTCG 120
MN121155.1:27-444      ACTACTGGAAACGGTAGCTAATACCGCATAACGTCGCAAGACCAAGAGGGGGACCTTCG 120
MH725718.1:35-443      ACTACTGGAAACGGTAGCTAATACCGCATAACGTCGCAAGACCAAGAGGGGGACCTTCG 120
MH725704.1:35-443      ACTACTGGAAACGGTAGCTAATACCGCATAACGTCGCAAGACCAAGAGGGGGACCTTCG 120
MH725703.1:35-443      ACTACTGGAAACGGTAGCTAATACCGCATAACGTCGCAAGACCAAGAGGGGGACCTTCG 120
*****

11F(this
KY780352.1:52-469      GGCCCTCTTGCCATCGGATGTGCCCAGATGGGATTAGCTAGTAGGTGGGGTAAACGGCTCAC 180
ON054402.1:45-462      GGCCCTCTTGCCATCGGATGTGCCCAGATGGGATTAGCTAGTAGGTGGGGTAAACGGCTCAC 180
MT573069.1:23-440      GGCCCTCTTGCCATCGGATGTGCCCAGATGGGATTAGCTAGTAGGTGGGGTAAACGGCTCAC 180
MT516163.1:34-451      GGCCCTCTTGCCATCGGATGTGCCCAGATGGGATTAGCTAGTAGGTGGGGTAAACGGCTCAC 180
MT114948.1:4-421       GGCCCTCTTGCCATCGGATGTGCCCAGATGGGATTAGCTAGTAGGTGGGGTAAACGGCTCAC 180
MN147831.1:22-438      GGCCCTCTTGCCATCGGATGTGCCCAGATGGGATTAGCTAGTAGGTGGGGTAAACGGCTCAC 180
MN121585.1:27-443      GGCCCTCTTGCCATCGGATGTGCCCAGATGGGATTAGCTAGTAGGTGGGGTAAACGGCTCAC 180
MN121155.1:27-444      GGCCCTCTTGCCATCGGATGTGCCCAGATGGGATTAGCTAGTAGGTGGGGTAAACGGCTCAC 180
MH725718.1:35-443      GGCCCTCTTGCCATCGGATGTGCCCAGATGGGATTAGCTAGTAGGTGGGGTAAACGGCTCAC 180
MH725704.1:35-443      GGCCCTCTTGCCATCGGATGTGCCCAGATGGGATTAGCTAGTAGGTGGGGTAAACGGCTCAC 180
MH725703.1:35-443      GGCCCTCTTGCCATCGGATGTGCCCAGATGGGATTAGCTAGTAGGTGGGGTAAACGGCTCAC 180
*****

```

Fig. (15): Multiple sequence alignment analysis of *Escherichia coli* (11F).

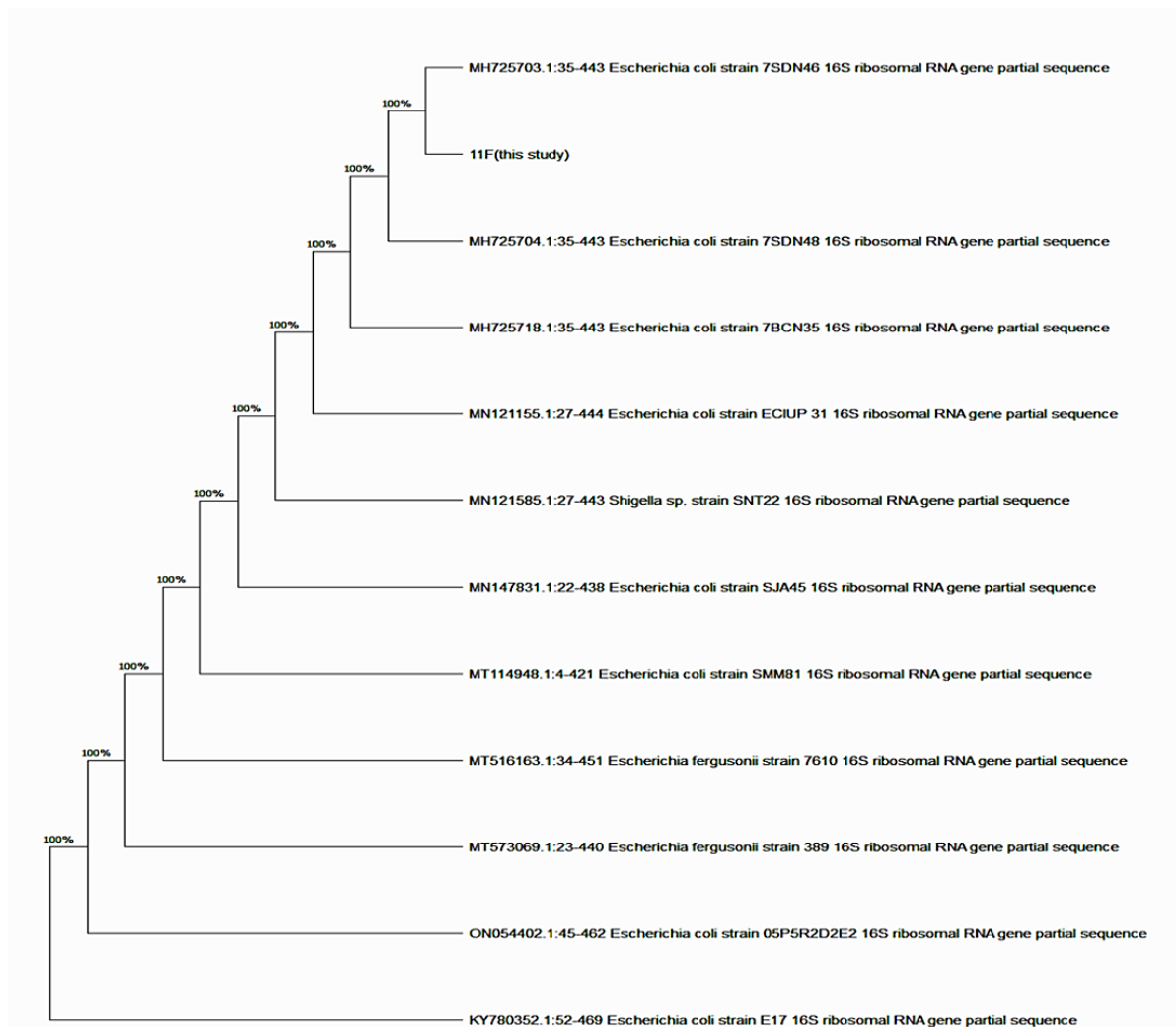


Fig. (16): Phylogenetic tree of *Escherichia coli* (11F).

Antibiotic susceptibility test (AST)

The antibiotic susceptibility test (AST) was done on the studied bacteria against some types of antibiotics based on CLSI (2022), and they were resistant to several antibiotics i.e. MDR bacteria as shown in table (3).

Antibacterial activity of AgNPs

The efficiency of silver nanoparticles generated by aqueous extract of the fruits of *A. esculentus* against three Gram-negative and one Gram-positive bacteria, all of which are antibiotic-resistant (MDR), was investigated in the current study. This was done with five different concentrations of AgNPs. The results demonstrated that these bacteria were sensitive to nanoparticles at all doses and more efficient

in Gram-positive than Gram-negative bacteria. While *Staphylococcus auricularis* (8F) had the lowest antibacterial activity at 1000 $\mu\text{g}\cdot\text{ml}^{-1}$, *Escherichia coli* (3R) was the most resistant to nanoparticles at all concentrations. As a result, the nanoparticles generated in the current study were more efficient against Gram-positive bacteria than Gram-negative bacteria. Also there is no statistically significant variation found between concentration of AgNPs and inhibition zone, and between bacterial species (Fig. 17). Same results were reported by (Shareef *et al.*, 2022; González- Pedroza *et al.*, 2023). In a separate study, Bruna *et al.* (2021) found that silver nanoparticles inhibit the growth of both Gram-negative and Gram-positive bacteria, as well as MDR bacteria.

They can also interact with the biomolecules present in the extract that were employed in the production of AgNPs. This might be due to the

biomolecules employed in the production of these particles.

Table (3): The antibiotic susceptibility test (AST) of the studied bacteria (*S. auricularis*).

Antibiotic	Antibiotic class	Antibiotic concentration (µg)	<i>S. auricularis</i> (8F)	<i>E. coli</i> (3R)	<i>A. faecalis</i> (2R)	<i>E. coli</i> (11F).
Amoxicillin-Clavulanate	β- Lactam combination agents	20/10	-	R	R	R
Ampicillin	Penicillins	10	-	S	R	R
Azithromycin	Macrolides	15	S	S	R	R
Aztreonam	Monobactams	30	-	-	R	R
Ceftazidime	Cephems	30	-	I	R	R
Chloramphenicol	Phenicols	30	S	S	R	S
Ciprofloxacin	Quinolones & Fluoroquinolones	5	S	S	R	R
Clindamycin	Lincosamides	2	-	R	-	-
Colistin	Lipopeptides	10	-	R	R	R
Fosfomycin	Fosfomycins	200	-	S	R	S
Gentamicin	Aminoglycosides	10	S	-	-	-
Linezolid	Oxazolidinones	30	S	-	-	-
Meropenem	Carbapenems	10	-	S	I	S
Methicillin	β- Lactam	5	10	-	-	-
Nitrofurantion	Nitrofurans	300	S	R	R	R
Penicillin	β- Lactam	10	-	R	-	-
Piperacillin	Penicillins	100	-	-	R	R
Piperacillin-tazobactam	β- Lactam combination agents	100/10	-	-	I	R
Rifampicin	Ansamycins	5	S	-	-	-
Teicoplanin	Lipoglycopeptides	30	I	-	-	-
Tetracycline	Tetracyclines	30	S	S	I	R
Trimethoprim-Sulfamethoxazole	Folate Pathway Antagonists	25 (1.25/23.75)	S	S	R	R
Vancomycin	Glycopeptides	30	S	-	-	-

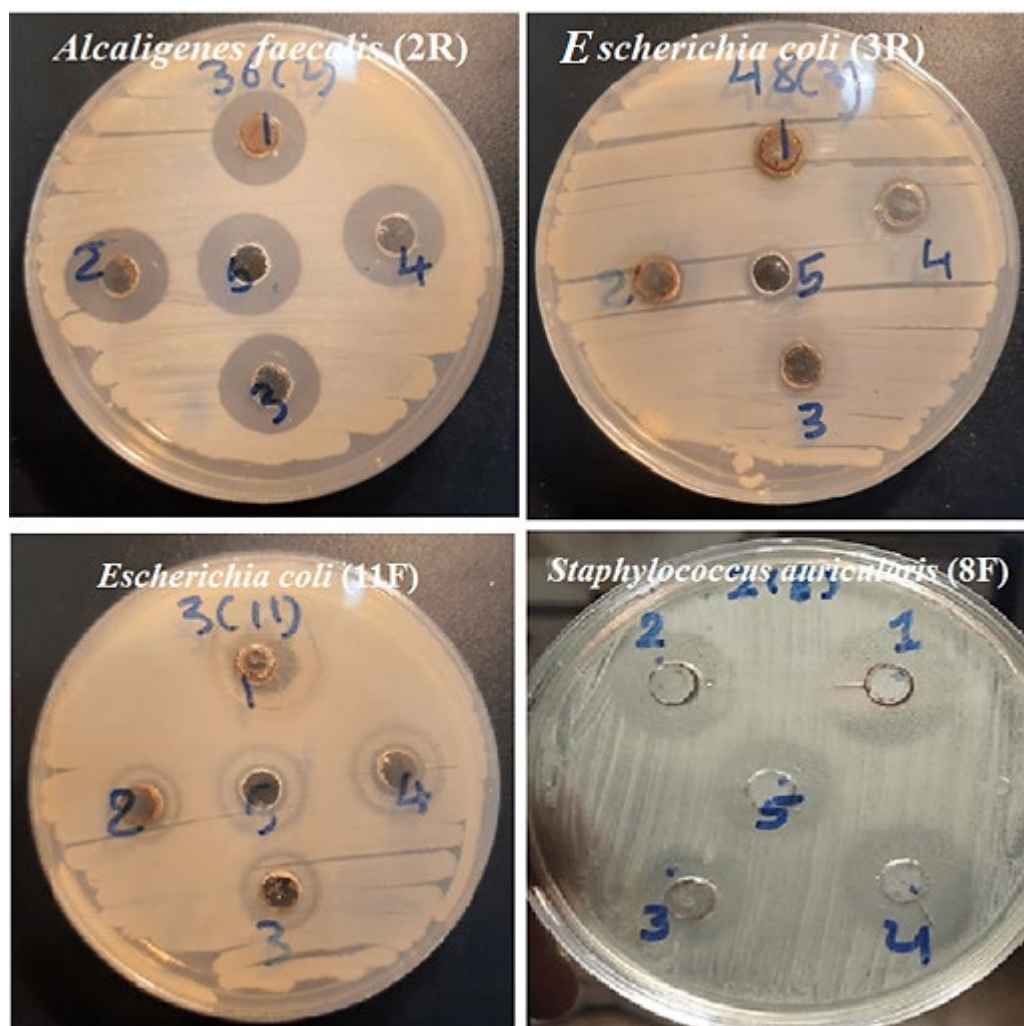


Fig. (17): Antibacterial activity of AgNPs (1:1000; 2:500; 3:250; 4:125; 5:62.5µg.ml⁻¹).

Synergistic action of AgNPs with antibiotics

The results of incorporating silver nanoparticles with some antibiotics revealed that the best synergy was recorded with the antibiotic Amoxicillin clavulanate (AMC) against all species of Gram-negative bacteria, with the highest rate of synergy against *Alcaligenes faecalis* (2R) where the percentage fold increase was 83% and FICI (2.2), followed by ciprofloxacin (CIP) with a percentage fold increase of 83% (FICI = 2.2) against 2R bacteria. Ampicillin has a 50% increase in percentage folds against 2R bacteria. In the case of the antibiotic Fosfomycin, the increase was 45% against 2R

bacteria. While the results of synergy against Gram-positive bacteria represented by 8F bacteria, the best percentage of synergy was the antibiotic vancomycin with a percentage of 13.3%, followed by the ciprofloxacin antibiotic with a percentage of 12.5%, and the least with the antibiotic Chloramphenicol with a percentage of 7.5%. On the other hand, no cases of antagonism were recorded with Gram-negative bacteria, but there was antagonism in the action of antibiotics and nanoparticles against gram-positive bacteria 8F with penicillin and methicillin antibiotics (Table 7, Fig. 18).

Table (4): Inhibition zone of AgNPs alone and AgNPs in combination with Antibiotics against *Alcaligenes faecalis* (2R).

Antibiotics	Antibiotics inhibition zone(mm)	Inhibition zone of AgNPs(mm)					Inhibition zone of AgNPs+ Antibiotics (mm)					Fractional inhibitory concentration index(FICI)					Percentage fold increases				
		AgNPs concentration					AgNPs concentration					AgNPs concentration					AgNPs concentration				
		1000 $\mu\text{g.ml}^{-1}$	500 $\mu\text{g.ml}^{-1}$	250 $\mu\text{g.ml}^{-1}$	125 $\mu\text{g.ml}^{-1}$	62.5 $\mu\text{g.ml}^{-1}$	1000 $\mu\text{g.ml}^{-1}$	500 $\mu\text{g.ml}^{-1}$	250 $\mu\text{g.ml}^{-1}$	125 $\mu\text{g.ml}^{-1}$	62.5 $\mu\text{g.ml}^{-1}$	1000 $\mu\text{g.ml}^{-1}$	500 $\mu\text{g.ml}^{-1}$	250 $\mu\text{g.ml}^{-1}$	125 $\mu\text{g.ml}^{-1}$	62.5 $\mu\text{g.ml}^{-1}$	1000 $\mu\text{g.ml}^{-1}$	500 $\mu\text{g.ml}^{-1}$	250 $\mu\text{g.ml}^{-1}$	125 $\mu\text{g.ml}^{-1}$	62.5 $\mu\text{g.ml}^{-1}$
Ampicillin (AMP)	15	11	10	10	10	10	15	16	16	15	15	1.73	1.6	1.56	1.67	1.67	0	6.67	6.67	0	0
Amoxicillin clavulanate (AMC)	6	11	10	10	10	10	7	7	8	7	6	2.43	2.3	2	2.29	2.67	16.7	16.7	33.3	16.7	0
Ciprofloxacin (CIP)	37	11	10	10	10	10	38	39	39	38	37	1.26	1.2	1.21	1.24	1.27	2.7	5.41	5.41	2.7	0
Chloramphenicol (C)	27	11	10	10	10	10	30	30	30	27	27	1.27	1.2	1.23	1.37	1.37	11.1	11.1	11.1	0	0
Fosfomycin (FO)	38	11	10	10	10	10	38	40	40	39	39	1.29	1.2	1.2	1.23	1.23	0	5.26	5.26	2.63	2.6

Chi-square test: non-significant at $p \leq 0.05$; $FICI \leq 0.5$ (synergy) or $FIC > 0.5 < 4$, (additive), and $FIC > 4$ (antagonism).

Table (5): Inhibition zone of AgNPs alone and AgNPs in combination with antibiotics against *Escherichia coli* (3R).

Antibiotics	Antibiotics inhibition zone(mm)	Inhibition zone of AgNPs (mm)					Inhibition zone of AgNPs+ Antibiotics (mm)					Fractional inhibitory concentration index (FICI)					Percentage fold increases%				
		AgNPs concentration					AgNPs concentration					AgNPs concentration					AgNPs concentration				
		1000 $\mu\text{g.ml}^{-1}$	500 $\mu\text{g.ml}^{-1}$	250 $\mu\text{g.ml}^{-1}$	125 $\mu\text{g.ml}^{-1}$	62.5 $\mu\text{g.ml}^{-1}$	1000 $\mu\text{g.ml}^{-1}$	500 $\mu\text{g.ml}^{-1}$	250 $\mu\text{g.ml}^{-1}$	125 $\mu\text{g.ml}^{-1}$	62.5 $\mu\text{g.ml}^{-1}$	1000 $\mu\text{g.ml}^{-1}$	500 $\mu\text{g.ml}^{-1}$	250 $\mu\text{g.ml}^{-1}$	125 $\mu\text{g.ml}^{-1}$	62.5 $\mu\text{g.ml}^{-1}$	1000 $\mu\text{g.ml}^{-1}$	500 $\mu\text{g.ml}^{-1}$	250 $\mu\text{g.ml}^{-1}$	125 $\mu\text{g.ml}^{-1}$	62.5 $\mu\text{g.ml}^{-1}$
Ampicillin (AMP)	6	18	18	19	19	20	9	8	8	6	6	2.67	3	3.13	4.17	4.33	50	33.3	33.3	0	0
Amoxicillin clavulanate (AMC)	6	18	18	19	19	20	11	11	10	8	8	2.18	2.2	2.5	3.13	3.25	83.3	83.3	66.7	33.3	33
Ciprofloxacin (CIP)	6	18	18	19	19	20	11	10	10	8	8	2.18	2.4	2.5	3.13	3.25	83.3	66.7	66.7	33.3	33
Chloramphenicol (C)	11	18	18	19	19	20	13	13	12	12	12	2.23	2.2	2.5	2.5	2.58	18.2	18.2	9.09	9.09	9.1
Fosfomycin (FO)	11	18	18	19	19	20	12	16	15	15	15	2.42	1.8	2	2	2.07	9.09	45.5	36.4	36.4	36

Chi-square test: non-significant at $p \leq 0.05$; $\text{FICI} \leq 0.5$ (synergy) or $\text{FIC} > 0.5 < 4$, (additive), and $\text{FIC} > 4$ (antagonism).

Table (6): Inhibition zone of AgNPs alone and AgNPs in combination with antibiotics against *Escherichia coli* (11F).

Antibiotics	Antibiotics inhibition zone(mm)	Inhibition zone of AgNPs(mm)					Inhibition zone of AgNPs+ Antibiotics(mm)					Fractional inhibitory concentration index(FICI)					Percentage fold increases				
		AgNPs concentration					AgNPs concentration					AgNPs concentration					AgNPs concentration				
		1000 $\mu\text{g}\cdot\text{ml}^{-1}$	500 $\mu\text{g}\cdot\text{ml}^{-1}$	250 $\mu\text{g}\cdot\text{ml}^{-1}$	125 $\mu\text{g}\cdot\text{ml}^{-1}$	62.5 $\mu\text{g}\cdot\text{ml}^{-1}$	1000 $\mu\text{g}\cdot\text{ml}^{-1}$	500 $\mu\text{g}\cdot\text{ml}^{-1}$	250 $\mu\text{g}\cdot\text{ml}^{-1}$	125 $\mu\text{g}\cdot\text{ml}^{-1}$	62.5 $\mu\text{g}\cdot\text{ml}^{-1}$	1000 $\mu\text{g}\cdot\text{ml}^{-1}$	500 $\mu\text{g}\cdot\text{ml}^{-1}$	250 $\mu\text{g}\cdot\text{ml}^{-1}$	125 $\mu\text{g}\cdot\text{ml}^{-1}$	62.5 $\mu\text{g}\cdot\text{ml}^{-1}$	1000 $\mu\text{g}\cdot\text{ml}^{-1}$	500 $\mu\text{g}\cdot\text{ml}^{-1}$	250 $\mu\text{g}\cdot\text{ml}^{-1}$	125 $\mu\text{g}\cdot\text{ml}^{-1}$	62.5 $\mu\text{g}\cdot\text{ml}^{-1}$
Ampicillin(AMP)	6	18	14	15	16	16	6	6	6	6	6	4	3.3	3.5	3.67	3.67	0	0	0	0	0
Amoxicillin clavulanate (AMC)	6	18	14	15	16	16	9	8	8	8	8	2.67	2.5	2.63	2.75	2.75	50	33.3	33.3	33.3	33
Ciprofloxacin (CIP)	9	18	14	15	16	16	10	10	10	9	9	2.7	2.3	2.4	2.78	2.78	11.1	11.1	11.1	0	0
Chloramphenicol (C)	30	18	14	15	16	16	32	33	33	31	32	1.5	1.3	1.36	1.48	1.44	6.67	10	10	3.33	6.7
Fosfomycin (FO))	37	18	14	15	16	16	39	39	38	37	37	1.41	1.3	1.37	1.43	1.43	5.41	5.41	2.7	0	0

Chi-square test: non-significant at $p \leq 0.05$; $FICI \leq 0.5$ (synergy) or $FIC > 0.5 < 4$, (additive), and $FIC > 4$ (antagonism).

Table (7): Inhibition zone of AgNPs alone and AgNPs in combination with antibiotics against *Staphylococcus auricularis* (8F).

Antibiotics	Antibiotics inhibition zone(mm)	Inhibition zone of AgNPs(mm)					Inhibition zone of AgNPs+ Antibiotics(mm)					Fractional inhibitory concentration index(FICI)					Percentage fold increases				
		AgNPs concentration					AgNPs concentration					AgNPs concentration					AgNPs concentration				
		1000 $\mu\text{g.ml}^{-1}$	500 $\mu\text{g.ml}^{-1}$	250 $\mu\text{g.ml}^{-1}$	125 $\mu\text{g.ml}^{-1}$	62.5 $\mu\text{g.ml}^{-1}$	1000 $\mu\text{g.ml}^{-1}$	500 $\mu\text{g.ml}^{-1}$	250 $\mu\text{g.ml}^{-1}$	125 $\mu\text{g.ml}^{-1}$	62.5 $\mu\text{g.ml}^{-1}$	1000 $\mu\text{g.ml}^{-1}$	500 $\mu\text{g.ml}^{-1}$	250 $\mu\text{g.ml}^{-1}$	125 $\mu\text{g.ml}^{-1}$	62.5 $\mu\text{g.ml}^{-1}$	1000 $\mu\text{g.ml}^{-1}$	500 $\mu\text{g.ml}^{-1}$	250 $\mu\text{g.ml}^{-1}$	125 $\mu\text{g.ml}^{-1}$	62.5 $\mu\text{g.ml}^{-1}$
Penicillin (P)	55	22	20	18	20	17	45	46	44	63	60	1.71	1.6	1.66	1.19	1.2	-18	-16.4	-20	14.5	9.1
Vancomycin (VAN)	30	22	20	18	20	17	33	34	32	30	32	1.58	1.5	1.5	1.67	1.47	10	13.3	6.6 7	0	6.7
Methicillin (MET)	20	22	20	18	20	17	11	11	20	18	19	3.82	3.6	1.9	2.22	1.95	-45	-45	0	-10	-5
Chloramphenicol (C)	40	22	20	18	20	17	40	43	42	41	41	1.55	1.4	1.38	1.46	1.39	0	7.5	5	2.5	2.5
Ciprofloxacin (CIP)	40	22	20	18	20	17	45	45	43	41	44	1.38	1.3	1.35	1.46	1.3	12.5	12.5	7.5	2.5	10

Chi-square test: non-significant at $p \leq 0.05$; $FICI \leq 0.5$ (synergy) or $FIC > 0.5 < 4$, (additive), and $FIC > 4$ (antagonism)

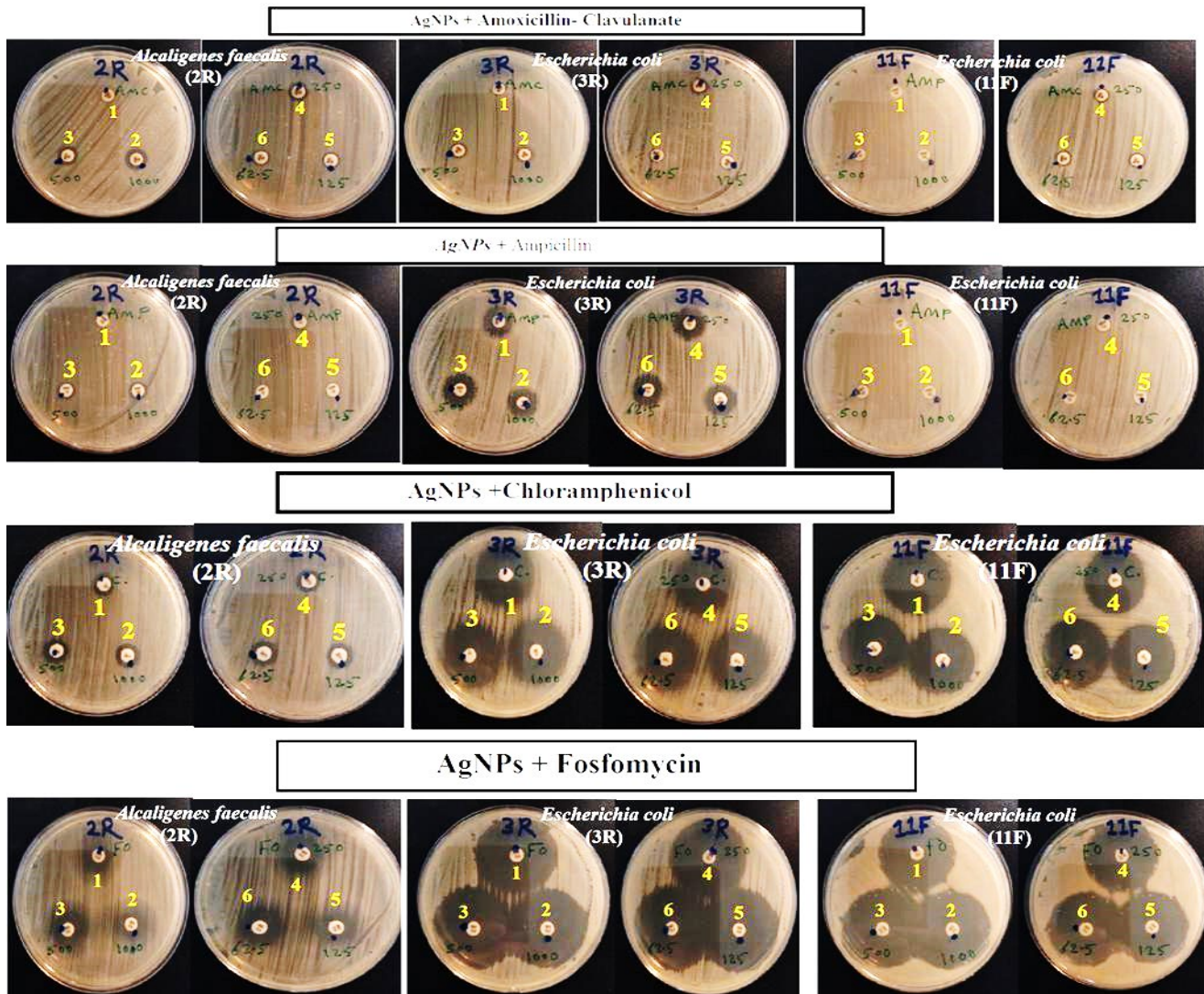


Fig. (18): Combination of AgNPs from *A. esculentus* fruit aqueous extract with Antibiotics: (1) Antibiotic alone, (2) Antibiotic+AgNPs (1000 µg.ml⁻¹), (3) Antibiotic+AgNPs (500 µg.ml⁻¹), (4) Antibiotic+AgNPs (250 µg.ml⁻¹), (5) Antibiotic+AgNPs (125 µg.ml⁻¹), (6) Antibiotic+AgNPs (62.5 µg.ml⁻¹).

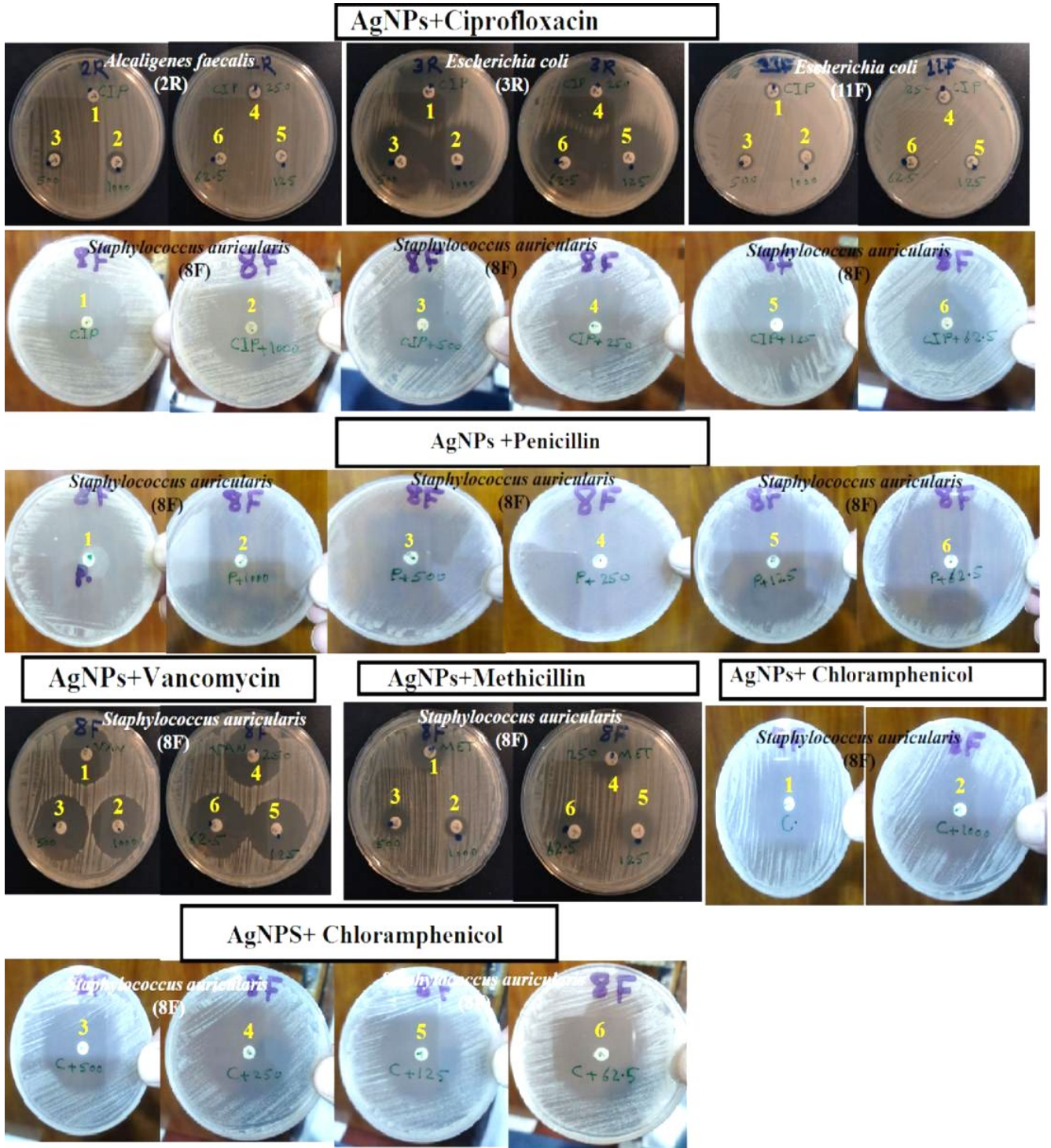


Fig. (18): (continued).

As a result, it can be concluded that the silver nanoparticles contributed to the enhancement of the activity of the majority of the antibiotics utilized in the present study. Hussein & Muslim (2019) reported identical results, observing a synergistic impact of silver nanoparticles added to some of the antibiotics, which led to enhancing the inhibitory activity of the two antibiotics, chloramphenicol and ciprofloxacin, against *S. aureus*. Khlaifat *et al.* (2019) found that chloramphenicol did not have a synergistic effect when mixed with silver nanoparticles against *E. coli* bacteria, and this is contrary to the results of the current study, where there was a synergistic effect of this antibiotic against *E. coli* bacteria. Many researchers have conducted many studies to determine the synergistic effect of silver nanoparticles when added to antibiotics, but the results of the synergy differ significantly from one study to the other, as some antibiotics improve their performance after addition, while others are inhibited and vice versa. The synergistic impact of silver nanoparticles and antibiotics may be due to an increase in antibacterial activity when silver nanoparticles are combined rather than AgNPs alone (Abdel-Wahab *et al.*, 2021).

The antibiotics resistant bacteria have become a serious problem because the bacteria's resistance to antibiotics increases faster than the process of developing new antibiotics to treat them, presenting a difficult problem for researchers and therapists in treating these bacteria, as well as the resulting increase in patients' bedtime in hospitals and the associated economic or financial burdens. Other bacteria may be acquired from certain hospitals, and thus the danger may be fatal. And thus arisen the need to create new antimicrobials in order to combat the problem of antibiotic-resistant bacteria. Because of

their particular properties that allow them to kill or inhibit bacteria that are resistant to antibiotics, silver nanoparticles appear to be the most effective option at present. The bacteriocidal effect of silver nanoparticles increases with decreasing particle size, since antibacterial activity is inversely related to nanoparticle size (Ankanna *et al.*, 2010). Experiments have demonstrated that biologically produced silver nanoparticles are more effective than those produced by other means. One probable mechanism for silver nanoparticle activity is that they interact with bacterial cell membrane proteins, affecting the permeability of that membrane. When silver ions adhere to the bacterial cell membrane, the charge of the membrane changes, and the cell components decompose. Furthermore, silver nanoparticles participate in conversion processes through the de phosphorylation of tyrosine residues, which results in bacterial cell starting steps programmed cell death. Immediately after entering the silver nanoparticles into the bacterial cell, they will bind with the enzymes of the respiratory chain, resulting in the disruption of ATP synthesis and potassium transport. In terms of the effect of silver nanoparticles on DNA, they lead its modification through the interaction of silver nanoparticles with sulfur and phosphorus groups of DNA, resulting in destroying the hydrogen bonds between the two strands of DNA, and thus stopping the process of DNA replication, leading to the cessation of growth. The silver nanoparticles can interact with RNA, resulting in the non-binding of the tRNA to the ribosome and the termination of the translation process of protein synthesis and glucose metabolism (Qing *et al.*, 2018; Kowalczyk *et al.*, 2021).

Conclusion

The antibacterial activity of AgNPs generated through the current study was evaluated against MDR bacteria. The findings revealed that these nanoparticles had good antibacterial activity against all bacteria tested, with Gram-negative bacteria being more vulnerable than Gram-positive organisms and it enhanced the antibacterial activity. Once combined with various antibiotics, they exhibited an excellent synergistic effect against all species of Gram-negative and Gram-positive bacteria, with the highest rate of synergy recorded against *Alcaligenes faecalis* (2R), where the percentage folds increase reached 83%.

Acknowledgments

The researchers would like to express their gratitude and appreciation to the Head of the Biology Department and the Deanship of the College of Education for Pure Sciences for providing the necessary resources for the current study.

Contributions of authors

A. A. S.: suggest a research topic, complete part of the practical side, and contribute to writing it.

F. J. F.: Contribute to providing samples and accomplish part of the practical side.

F. A. A.: Contribute in part from the practical side and the interpretation of some of the results.

ORCID

A.A.S.: <https://orcid.org/0000-0002-3545-0349>

F. J. F., <https://orcid.org/0000-0002-4130-8840>

F.A. A. A., <https://orcid.org/0000-0002-9933-9252>

Conflicts of interest

The authors declare that they have no conflict of interests.

References

- Abdel-Wahab, F., El Menofy, N., El- Batal, A., Mosallam, F., & Abdulall, A. (2021). Enhanced antimicrobial activity of the combination of silver nanoparticles and different β Lactam antibiotics against methicillin resistant *Staphylococcus aureus* isolates. *Azhar International Journal of Pharmaceutical and Medical Sciences*, 1(1), 22-31. <https://doi.org/10.21608/ajpms.2021.53610.1017>
- Akintelu, S. A., Folorunso, A. S., Folorunso, F. A., & Oyebamiji, A. K. (2020). Green synthesis of copper oxide nanoparticles for biomedical application and environmental remediation. *Heliyon*, 6(7), e04508 <https://doi.org/10.1016/j.heliyon.2020.e04508>
- Alaqad, K. & Saleh, T. A. (2016). Gold and silver nanoparticles: synthesis methods, characterization routes and applications towards drugs. *Journal of Environmental & Analytical Toxicology*, 6, 1-10.
- Almudhafar, S. M. A., & Al-Hamdani, M. A. (2022). Antibacterial and Anticancer effects of silver nanoparticles synthesised using *Eragrostis tef* and *Vitellaria paradoxa* seeds extract. *Basrah Journal of Agricultural Sciences*, 35(2), 132–159. <https://doi.org/10.37077/25200860.2022.35.2.10>
- Al-Musawi, Z. F. H., & Al-Saadi, N. H. M. (2021). Antitumor activities of biosynthesized silver nanoparticles using *Dodonaea viscosa* (L.) leaves extract. *Basrah Journal of Agricultural Sciences*, 34(2), 42–59. <https://doi.org/10.37077/25200860.2021.34.2.04>
- Ankanna, S., Prasad, T.N.V.K.V., Elumalai, E. K., & Savithamma, N. (2010). Production of biogenic silver nanoparticles using *Boswellia ovalifoliolata* stem bark. *Digest Journal of Nanomaterials and Biostructures*, 5, 369-372.
- Balavijayalakshmi, J., & Ramalakshmi, V. (2017). *Carica papaya* peel mediated synthesis of silver nanoparticles and its antibacterial activity against human pathogens. *Journal of Applied Research and Technology*, 15(5), 413–422.
- Bruna, T., Maldonado-Bravo, F., Jara, P., & Caro, N. (2021). Silver Nanoparticles and Their Antibacterial Applications. *International Journal of Molecular Sciences*, 22(13), 7202. <https://doi.org/10.3390%2Fijms22137202>
- Chakravarty, H. L. (1976). *Plant wealth of Iraq*. Ministry of Agriculture and Agrarian Reform,

- Baghdad, 304pp.
<https://catalogue.nla.gov.au/Record/1505572>
- González-Pedroza, M. G., Benítez, A. R. T., Navarro-Marchal, S. A., Martínez-Martínez, E., Marchal, J. A., Boulaiz, H., & Morales-Luckie, R. A. (2023). Biogeneration of silver nanoparticles from *Cuphea procumbens* for biomedical and environmental applications. *Scientific Reports*, 13(1), 790.
<https://doi.org/10.1038/s41598-022-26818-3>
- Habeeb Rahuman, H. B., Dhandapani, R., Narayanan, S., Palanivel, V., Paramasivam, R., Subbarayalu, R., Thangavelu, S., & Muthupandian, S. (2022). Medicinal plants mediated the green synthesis of silver nanoparticles and their biomedical applications. *Institution of Engineering and Technology*, 16(4), 115-144.
<https://doi.org/10.1049/nbt.12078>
- Hussein, N. N., & Muslim, H. (2019). Detection of the antibacterial activity of AgNPs biosynthesized by *Pseudomonas aeruginosa*. *Iraqi Journal of Agricultural Sciences*, 50(2), 617-625.
<https://jcoagri.uobaghdad.edu.iq/index.php/intro/article/view/661>
- Jemal, K., Sandeep, B. V., & Pola, S. (2017). Synthesis, characterization, and evaluation of the antibacterial activity of *allophylus serratus* leaf and leaf derived callus extracts mediated silver nanoparticles. *Journal of Nanomaterials*, 2017, Article ID 4213275, 1-11.
<https://doi.org/10.1155/2017/4213275>
- Khlaifat, A. M., Al-limoun, M. O., Khleifat, K.M., Al Tarawneh, A. A., Qaralleh, H., Rayyan, E. A., & Alsharafa, K. Y. (2019). Antibacterial synergy of *Tritirachium oryzae*-produced silver nanoparticles with different antibiotics and essential oils derived from *Cupressus sempervirens* and *Asteriscus graveolens* (Forssk). *Tropical Journal of Pharmaceutical Research*, 18(12), 2605-2615
<https://www.ajol.info/index.php/tjpr/article/view/211138>
- Kowalczyk, P., Szymczak, M., Maciejewska, M., Laskowski, Ł., Laskowska, M., Ostaszewski, R., Skiba, G. & Franiak-Pietryga, I. (2021). All that glitters is not silver- a new look at microbiological and medical applications of silver nanoparticles. *International Journal of Molecular Sciences*, 22(2), 854. <https://doi.org/10.3390/ijms22020854>
- Moteriya, P., Padalia, H., & Chanda, S. (2017). Characterization, synergistic antibacterial and free radical scavenging efficacy of silver nanoparticles synthesized using *Cassia roxburghii* leaf extract. *Journal of Genetic Engineering and Biotechnology*, 15(2), 505–513.
<https://doi.org/10.1016/j.jgeb.2017.06.010>
- Norman, R. O. C. (1993). *Principles of Organic Synthesis*. 3rd ed. Routledge.
<https://doi.org/10.1201/9780203742068>
- Odds, F. C. (2003). Synergy, antagonism, and what the chequer board puts between them. *Journal of Antimicrobial Chemotherapy*, 52(1), 1–1.
<https://doi.org/10.1093/jac/dkg301>
- Praba, P., Vasantha, V.S., Jeyasundari, J., & Y. Jacob, B.A. (2015). Synthesis of plant-mediated silver nanoparticles using *Ficus microcarpa* leaf extract and evaluation of their antibacterial activities. *European Chemical Bulletin*, 4(3), 117–120.
- Qing, Y., Cheng, L., Ruiyan, L., Liu, G., Zhang, Y., Tang, X., Wang, J., Liu, H., & Qin, Y. (2018). Potential antibacterial mechanism of silver nanoparticles and the optimization of orthopedic implants by advanced modification technologies. *International Journal of Nanomedicine*, 13, 3311-3327. <https://doi.org/10.2147/IJN.S165125>
- Schuphan, I. (1974). Zum metabolismus von phenylharnstoff: III. Metabolismus von monolinuron-O-methyl 14C in chlorella pyrenoidosa, *Chemosphere*, 3(3), 131–134.
[https://doi.org/10.1016/0045-6535\(74\)90065-4](https://doi.org/10.1016/0045-6535(74)90065-4)
- Shareef, A.A., Hassan, Z.A., Kadhim, M.A., & Al-Mussawi, A.A. (2022). Antibacterial Activity of Silver Nanoparticles Synthesized by Aqueous Extract of *Carthamus oxycantha* M. Bieb. Against Antibiotics Resistant Bacteria. *Baghdad Science Journal*, 6, 19(3), 0460.
<https://bsj.uobaghdad.edu.iq/index.php/BSJ/article/view/5339>
- Tian, S., Hu, Y., Chen, X., Liu, C., Xue, Y., & Han, B. (2022). Green synthesis of silver nanoparticles using sodium alginate and tannic acid: characterization and anti-*S. aureus* activity. *International Journal of Biological Macromolecules*, 195, 515-522.
<https://doi.org/10.1016/j.ijbiomac.2021.12.031>
- Townsend, C. C., & Guest, E. (1980). *Flora of Iraq*. Vol. 4. (1) *Cornaceae to Rubiaceae*. Ministry of Agriculture and Agrarian Reform, Baghdad. 627pp.

Vanlalveni, C., Lallianrawna, S., Biswas, A., Selvaraj, M., Changmai, B., & Rokhum, S. L. (2021). Green synthesis of silver nanoparticles using plant extracts and their antimicrobial activities: a review of recent literature. *Royal Society of Chemistry Advances*, 11(5), 2804–2837.
<https://doi.org/10.1039/D0RA09941D>

Zahoor, M., Nazir, N., Iftikhar, M., Naz, S., Zekker, I., Burlakovs, J., Uddin, F., Kamran, A. W., Kallistova, A., Pimenov, N., & Ali Khan, F. A. (2021). Review on Silver nanoparticles: classification, various methods of synthesis, and their potential roles in biomedical applications and water treatment. *Water*, 13(16), 2216.
<https://doi.org/10.3390/w13162216>

الفعالية ضد بكتيرية لدقائق الفضة النانوية المصنعة بواسطة المستخلص المائي لثمار نبات *Abelmoschus esculentus* (L.) Moench بمفردها أو بإضافتها الى المضادات الحيوية

علي عبود شريف¹ وفاضل جبار فرحان² وفله عبدالستار عبد الرياحي¹

¹قسم علوم الحياة، كلية التربية للعلوم الصرفة، جامعة البصرة، العراق.

²قسم علوم البحار الطبيعية، كلية علوم البحار، جامعة البصرة، العراق.

المستخلص: تزداد تطبيقات الدقائق النانوية يوما بعد يوم نتيجة للخصائص الفريدة التي تمتلكها تلك الدقائق، والتي جذبت انتباه الباحثين ، ومن بين هذه التطبيقات استخدامها في تثبيط البكتيريا المقاومة للمضادات الحيوية. تهدف الدراسة الحالية إلى التخليق الحيوي لدقائق الفضة النانوية من ثمار نبات البامية *Abelmoschus esculentus* (L.) Moench، واختبار نشاطها المضاد للبكتيريا بمفردها أو بإضافتها الى بعض المضادات الحيوية. تم التأكد من تكون دقائق الفضة النانوية بواسطة تغير لون خليط التفاعل من اللون الأخضر الفاتح إلى البني الداكن. بالإضافة إلى استخدام طرق التحليل الطيفي لإثبات إنتاج هذه الدقائق، مثل UV-vis و FTIR و XRD و EDX. تم استخدام الفحص المجهر الإلكتروني (SEM) لتحديد اشكال وأحجام الدقائق النانوية المصنعة بالدراسة الحالية. تم اختبار الفعالية ضد بكتيرية لدقائق الفضة النانوية المصنعة في هذه الدراسة بمفردها أو بإضافتها الى بعض المضادات الحيوية. بينت النتائج ان لهذه الدقائق القدرة على تثبيط أربعة أنواع من البكتيريا المقاومة للمضادات الحيوية MDR، ثلاثة منها سالبة لصبغة كرام والرابعة كانت موجبة لصبغة كرام. أظهرت النتائج ايضا أن هذه البكتيريا تم تثبيطها عند استخدام دقائق الفضة النانوية بجميع التركيزات بمفردها أو عند اضافتها الى بعض المضادات الحيوية، ووجد أن AgNPs كانت أكثر فعالية ضد البكتيريا موجبة كرام من البكتيريا سالبة كرام. حيث كانت *Staphylococcus auricularis* (8F) أكثر أنواع البكتيريا حساسية، بينما كانت *Escherichia coli* (3R) أكثر أنواع البكتيريا مقاومة. أظهرت نتائج مزج دقائق الفضة النانوية مع بعض المضادات الحيوية ان أفضل تآزر عند خلط AgNPs مع المضاد الحيوي Amoxicillin clavulanate ضد جميع أنواع البكتيريا سالبة كرام، يليه Fosfomycin، و Ampicillin، ciprofloxacin.

الكلمات المفتاحية: دقائق الفضة النانوية، الفعالية ضد بكتيرية، التآزر مع المضادات الحيوية.